People's Democratic Republic of Algeria
Ministry of Higher Education and Scientific Research

University M'Hamed BOUGARA – Boumerdes

Institute of Electrical and Electronic Engineering

Department of Electronics

Final Year Project Report Presented in Partial Fulfilment of the Requirements for the Degree of

MASTER

In **Telecommunication**

Option: **Telecommunications**

Title:

Design of a Metamaterial Dual-band Bandpass Filter for WiMAX Applications

Presented by:

- **Debili Seif El Islam**
- **Zaboub Oussama**

Supervisor:

Pr.M.Challal

Registration Number:……../2020

Acknowledgments

First and foremost, we would like to thank almighty ALLAH for giving us the courage and the strength and the determination as well as guidance in conducting this project study, despite the difficulties.

Our sincere thanks and guidance goes to our supervisor and principal lecturer Prof.M.Chaalal for his support , guidance and encouragement during this project . His careful editing contributed enormously to accomplish this work.

We would like to express our sincere gratitude to Dr.F.Mouhouche , for the help and the support she provided during this research work .

Next, we owe a special thanks to the members of the jury who have agreed to evaluate our work.

Last but not least, many thanks go to all institute's teachers who have contributed directly or indirectly to our five-year journey in the institute.

Abstract

This work suggests the design of a dual-band bandpass filter (BPF) based on metamaterial triangular split ring cell. The proposed structure is designed using CST software . It is found that the suggested structure is developed to have two passbands at central frequencies 3.5 GHz and 5.8 GHz intended for WiMAX communication system. The design was performed in FR4 substrate with relative dielectric constant of 4.3, thickness of 1.63 mm and a dialectic loss tangent of 0.017 , the software used is CST microwave studio ..

Table of Contents

List of Figures

List of tables

List of abbreviations

BPF	Band Pass Filter
BW	Bandwidth
CST	Computer Simulation Technology
DPS	Double Positive
DNG	Double Negative
ENG	Epsilon Negative
FBW	Fractional Bandwidth
FR4	Flame Retardant 4
HPF	High Pass Filter
LPF	Low Pass Filter
MNG	Mu Negative
MW	Microwave
NIM	Negative Refractive Index Metamaterial
RF	Radio Frequency
SRR	Split Ring Resonator
WiMAX	Worldwide Interoperability for Microwave Access
WLAN	Wireless Local Area Network

List of symbols

wl	Strip line width
β	Propagation constant
θ	Electrical length
c	Light velocity
ε_{eff}	Effective dielectric constant
ε_r	Relative Permittivity
C	Capacitance
L	Inductance
R	Resistance
Z	Impedance
f_0	Center frequency
S_{ij}	Scattering parameters
f	Operating frequency
Hz	Hertz
dB	Decibel
H	Henry
F	Farad

Introduction

the development of microwave filter technology always depended on the requirements of the applications. Military applications in ,world war II and beyond , required wide-band and tunable devices for electronic support measures receivers, which led to the development of highly selective wide-band waveguide filters, coaxial resonator and suspended-substrate multiplexers, and electronically tunable filters. [1]

Then the satellite communications industry which began in the late 1960s created demand for low-mass narrow-band low-loss filters with severe specifications on amplitude selectivity and phase linearity. These requirements resulted in the development of dual-mode waveguide and dielectric-resonator filters, and advances in the design of contiguous multiplexers. [2]

Cellular communications base-stations demanded low-loss high power-handling selective filters with small physical size, capable of being manufactured in tens of thousands at a reasonable cost. These demands led to advances in coaxial resonator, dielectric resonator, and superconducting filters, and also to methods of cost-reduction, including computer-aided alignment. [2]

Recent development in wireless communication systems has presented new challenges to design and produce high-quality miniature components with a dual-band operation. Currently, one of the most desired objectives by the wireless communications industry is to improve the electrical performance of microwave filters, including bandpass filters (BPFs). These types of filter are frequently used in modern communication devices. Recent works on this kind of filter show a great development in the microwave filtering qualities, such as the miniaturization, selectivity and tunablility of the filters. A new class of physical devices can meet the needs of the performance of microwave systems; these devices are named “Metamaterials”.[3]

Metamaterials are pseudo-homogeneous structure having new physical characteristics. They are made by artificial structures of unit cells which are arranged in periodic way. These cells are at the scale smaller than wavelength of operating frequency. Many benefits like blocking, absorbing, enhancing, or bending of electromagnetic (EM) waves which are not possible in conventional material are achieved by metamaterials.[3]

In this master’s report, a design of compact dual-band BPF using metamaterials is introduced. This type of filter will be used for WiMAX communication system applications.

The first chapter presents the basic theory and application of the filters. Then, in the second one, metamaterials along with their properties and types are investigated. In the last chapter, the design development process in many steps is presented. Finally, a conclusion and some suggestions for future scope are presented.

Chapter 1

Theory of filters

Chapter 1 : Theory of filters

1.1 Introduction to filters

Filters are necessary to the operation of most electronic circuits. It is therefore in the interest of anyone involved in electronic circuit design to have the ability to develop filter circuits capable of meeting a given set of specifications. Unfortunately, many in the electronics field are uncomfortable with the subject, whether due to a lack of familiarity with it, or a reluctance to grapple with the mathematics involved in a complex filter design. This chapter is intended to serve as a very basic introduction to some of the fundamental concepts and terms associated with filters. This chapter will also introduce the concept of metamaterials which are artificial materials designed to achieve electromagnetic properties that are not available in nature.[4]

1.2 Types of filters

1.2.1 Low pass Filter

The first filter type is the low-pass. A low-pass filter passes low frequency signals, and rejects signals at frequencies above the filter's cutoff frequency. An example might be in a light-sensing instrument using a photodiode. If light levels are low, the output of the photodiode could be very small, allowing it to be partially obscured by the noise of the sensor and its amplifier, whose spectrum can extend to very high frequencies. If a low-pass filter is placed at the output of the amplifier, and if its cutoff frequency is high enough to allow the desired signal frequencies to pass, the overall noise level can be reduced. A number of low-pass filter amplitude response curves are shown in Figure (1-1) [4].

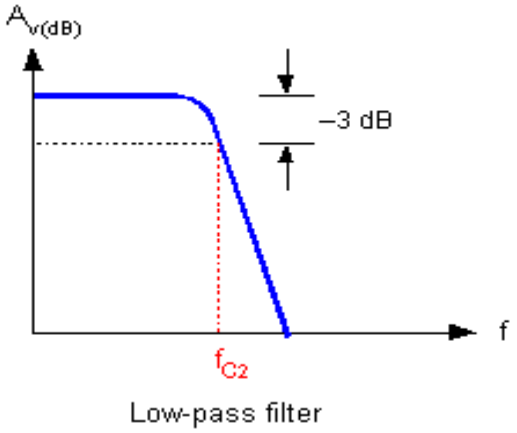

Figure 1-1 Examples of Lowpass filter amplitude responses

1.2.2 High pass filter

The opposite of the low-pass is the high-pass filter, which rejects signals below its cutoff frequency. One such application is in high fidelity loudspeaker systems. Music contains significant energy in the frequency range from around 100 Hz to 2 kHz, but high-frequency drivers (tweeters) can be damaged if low frequency audio signals of sufficient energy appear at their input terminals. A high-pass filter between the broadband audio signal and the tweeter input terminals will prevent low frequency program material from reaching the tweeter. In conjunction with a low-pass filter for the low-frequency driver (and possibly other filters for other drivers), the high-pass filter is part of what is known as a “crossover network” [4].

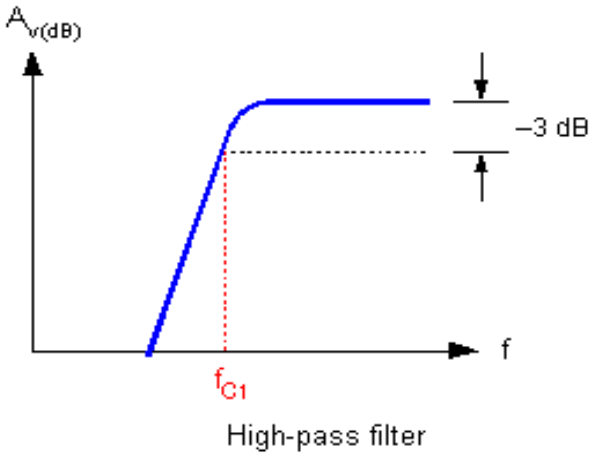

Figure 1-2 examples of high-pass filter amplitude responses

1.2.3 Band pass filter

It only lets through a certain determined frequency band (it attenuates everything above or below this band), an ideal response characteristic figure (1-3-a) that has absolutely constant gain within the passband, zero gain outside the passband, and an abrupt boundary between the two is impossible to realize in practice, but it can be approximated to varying degrees of accuracy by real filters. Curves (b) through (f) in figure (1-3) are examples of few band-pass amplitude response curves that approximate the ideal curves with varying degrees of accuracy. Note that while some band-pass responses are very smooth, other have ripple (gain variations in their passbands. Other have ripple in their stopbands as well. The stopband is the range of frequencies over which unwanted signals are attenuated. Band-pass filters have two stopbands, one above and one below the passband [4].

The rate of change of attenuation between the passband and the stopband also differs from one filter to the next. The slope of the curve in this region depends strongly on the order of the filter, with higher-order filters having steeper cutoff slopes. The attenuation slope is usually expressed in dB/octave (an octave is a factor of 2 in frequency) or dB/decade (a decade is a factor of 10 in frequency). Band-pass filters are used in electronic systems to separate a signal at one frequency or within a band of frequencies from signals at other frequencies [4].

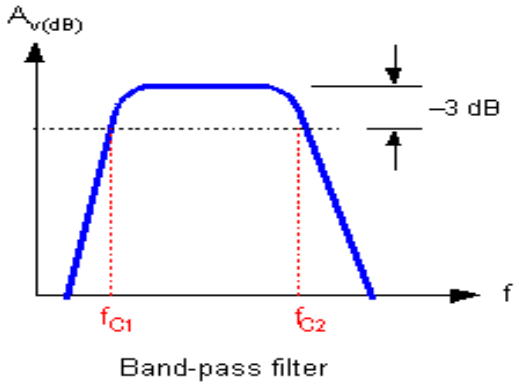

Figure 1-3 Examples of band-pass filter amplitude responses

1.2.4 Notch or band reject filter

A filter with effectively the opposite function of the band-pass is the band-reject or notch filter. Notch filters are used to remove an unwanted frequency from a signal, while affecting all other frequencies as little as possible. An example of the use of a notch filter is with an audio program that has been contaminated by 60 Hz power-line hum. A notch filter with a center frequency of 60 Hz can remove the hum while having little effect on the audio signals. A number of notch filter amplitude response curves are shown in Figure (1-4) [4].

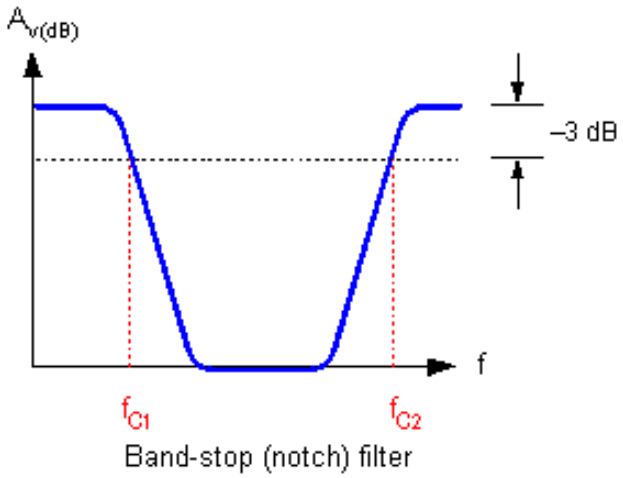

Figure 1-4 Examples of band-stop filters amplitude responses

1.3 The Scattering parameters

Scattering parameters or S-parameters (the elements of a scattering matrix or S-matrix) Describe the electrical behavior of liner electrical networks When undergoing various steady state stimuli by electrical signals. The parameters are useful for several branches of electrical engineering, including electronics, communication systems, and especially for microwave engineering [7].

In the context of S-parameters, scattering refer to the way in which the traveling currents and voltage in a transmission line are affected when they meet a discontinuity caused by

the insertion of a network into the transmission line. This is equivalent to the wave meeting an impedance differing from the line's characteristic impedance.

Although applicable at any frequency, S-parameters are mostly used for networks operating at radio frequency (RF) and microwave frequencies where signal power and energy considerations are more easily qualified than currents and voltages.

S-parameters are readily represented in matrix from and obey the rules of matrix algebra. Figure 1-5 represents two ports S-parameter network [6].

Figure 1-5 S-parameters two ports network

In this case the relationship between the reflected, incident power waves and the S-parameter matrix is given by [3]:

$$\begin{pmatrix} b_1 \\ b_2 \end{pmatrix} = \begin{pmatrix} S_{11} & S_{12} \\ S_{21} & S_{22} \end{pmatrix} \begin{pmatrix} a_1 \\ a_2 \end{pmatrix}$$

Expanding the matrices into equations gives:

$$b_1 = S_{11}a_1 + S_{12}a_2 \qquad (1-1a)$$

$$b_2 = S_{21}a_1 + S_{22}a_2 \qquad (1-1b)$$

If $a_2 = 0$, then $b_1 = S_{11}a_1$, so S11 can be defined as:

$$S_{11} = \left.\frac{b_1}{a_1}\right|_{a_2=0}$$

If $a_2 = 0$, $b_2 = S_{21}\, a_1$. So S_{21} can be defined as:

$$S_{21} = \left.\frac{b_2}{a_1}\right|_{a_2=0}$$

The 2-port S-parameters have the following generic description:

- S_{11} is the input port reflection coefficient.
- S_{21} is the forward transmission (insertion) gain.

1.4 Filter parameters

Response curves are used to describe how a filter behaves. A response curve is simply a graph showing an attenuation ratio (Vout / Vin) versus frequency (see Figure 1-6 below). Attenuation is commonly expressed in units of decibels (dB). Frequency can be expressed in two forms: either the angular form ω (units are rad/s) or the more common form of f (units of Hz, i.e., cycles per second). These two forms are related by $\omega = 2\pi f$. Finally, filter response curves may be plotted in linear-linear, log-linear, or log-log form. The most common approach is to have decibels on the y-axis and logarithmic frequency on the x-axis [8].

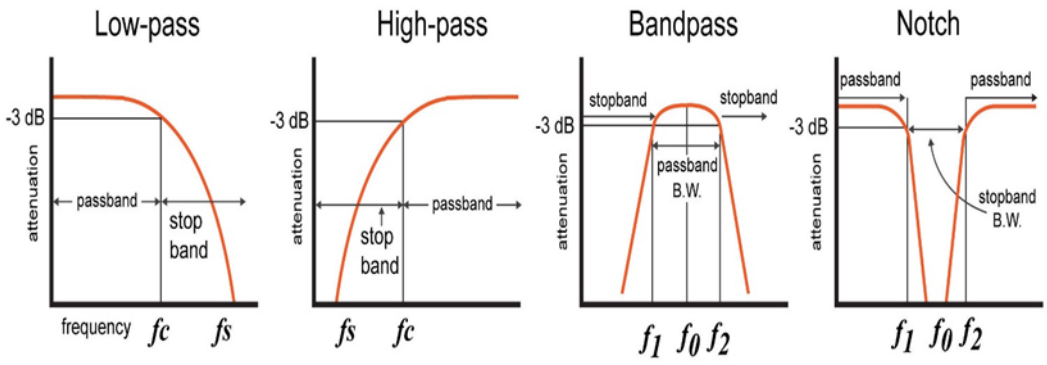

Figure 1-6 Response curves for the four major filter types.

Note: A notch filter is a band-stop filter with a narrow band-stop bandwidth. Notch filters are used to attenuate a narrow range of frequencies.

Below are some technical terms that are commonly used when describing filter response curves:

1.4.1 Transfer function

Transfer function are commonly used in the analysis of systems such as single-input and output filters, typically within the fields of signal processing, communication theory, and control theory.

The transfer function of a two-port filter network describes mathematically the characteristics of the network response an expression of S_{21}.Usually, an amplitude-squared transfer function for a lossless passive filter network is defined as [8]:

$$|S_{21}(jw)|^2 = \frac{1}{1+\varepsilon^2 F_n{}^2(w)} \qquad (1-2)$$

Where ε is the ripple constant, $F_n(w)$ represents a characteristic or filtering function, and w is a frequency variable[6].

1.4.2 Insertion Loss (L_A)

Is a measure of how much the filter attenuates a signal at a given frequency Numerically, the insertion loss of a filter is the ratio of the signal level at the input to the filter to the signal level at the output of the filter. The ability of the filter to remove unwanted noise from a circuit is called its insertion loss. Filter insertion loss if frequency-dependent, often changing several orders of magnitude over the filter's useful frequency range, so it is convenient to express insertion loss in units of decibels (dB).

$$L_A(db) = -20\log\left(\frac{unfiltered\ filter\ amplitude}{filtered\ filter\ amplitude}\right) = -20\log(|S_{21}|) \qquad (1-3)$$

Where S_{21} is the transmission coefficient of the filter

1.4.3 Return loss (Lr)

A filter performance characteristic providing the relative amount of power reflected by an input signal. Mathematically,

$$Return\ Loss\ =\ Lr\ = -20\log(|S_{11}|) = -20log\ (\frac{VSWR-1}{VSWR+1}) \qquad (1-4)$$

Where S_{11} is the reflection coefficient and VSWR is in a perfect transmission line, there is no reflected power so Return Loss is essentially infinite. In a perfectly reflective circuit, Return Loss is zero.

1.4.4 Bandwidth

Bandwidth in hertz is an important concept in different fields: electronics, digital communications, information theory, signal processing, ratio communications and spectroscopy.

In determines the capacity of a given communication channel. The bandwidth is the difference between the upper and the lower frequencies in a continuous set of frequencies relative to 3 dB attenuation point. It is the expressed as follows:

$$\mathrm{BW}(Hz) = f_{-3dB(upper)} - f_{-3dB(lower)} \qquad (1-5)$$

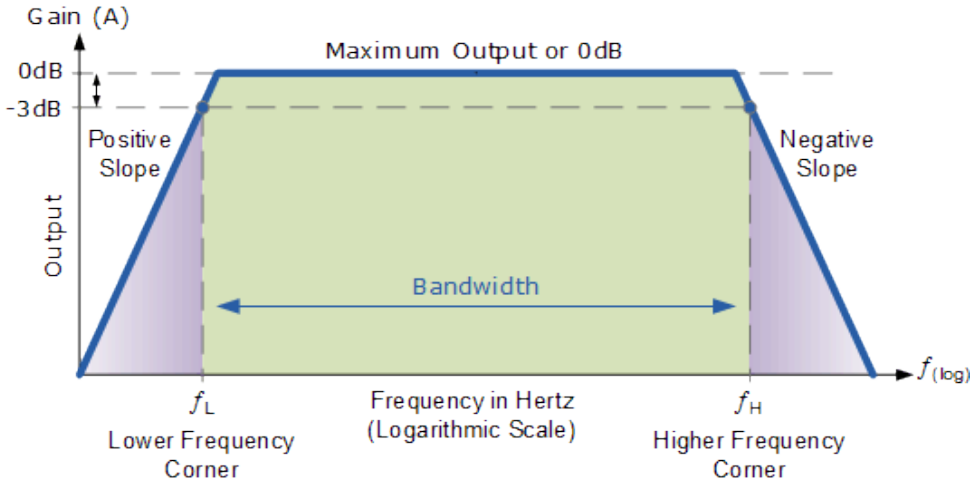

Figure 1-7 3dB bandwidth illustrated between the upper and the lower frequencies f_H and f_L.

1.4.5 Central Frequency

The center frequency of a filter or channel is a measure of a central frequency between the upper and lower cutoff frequencies. It is defined as either the arithmetic or the geometric mean of the lower cutoff frequencies.

The geometric mean value is the calculated as follows:

$$f_0(Geometric) = \sqrt{f_{-3dB_{upper}} \times f_{-3dB_{lower}}} \qquad (1-6)$$

The arithmetic mean value is the calculated as follows:

$$f_0(arithmetic) = \frac{\sqrt{f_{-3dB_{upper}} + f_{-3dB_{lower}}}}{2} \qquad (1-7)$$

1.4.6 Cutoff Frequency

A filter performance characteristic providing the end or start of the passband in Lowpass and High pass filters. For Lowpass filters, Fc specifies the upper passband edge or knee. For High pass filters, Fc specifies the lower passband edge.

1.4.7 Fractional bandwidth

Fractional bandwidth is the bandwidth of a device divided by its center frequency (f_H

and f_L are shown in figure 1-7)

It is calculated using the following formula:

$$\text{FBW}(\%) = \frac{f_H - f_L}{f_0} \times 100\% \qquad (1-8)$$

Where $f_0 = \frac{f_H - f_L}{2}$

1.4.8 Quality factor

The quality factor of a filter conveys its damping characteristics. In the time domain, damping corresponds to the amount of oscillation in the system's step response. In the frequency domain, higher Q corresponds to more (positive or negative) peaking in the system's magnitude response. For a bandpass or notch filter, Q represents the ratio between the center frequency and the -3dB bandwidth (i.e., the distance between f_H and f_L).

For both band-pass and notch filters:

$$Q = \frac{f_0}{(f_H - f_L)} \qquad (1-9)$$

1.4.9 All-pass or phase -shift filter

The fifth and final filter response type has no effect on the amplitude of the signal at different frequencies. Instead, its function is to change the phase of the signal without affecting its amplitude. This type of filter is called an all-pass or phase-shift filter. All-pass filters are typically used to introduce phase shifts into signals in order to cancel or partially cancel any unwanted phase shifts previously imposed upon the signals by other circuitry or transmission media

1.4.10 Application

In the field of electronics, there are many practical applications for filters. Examples include:

- **Radio communications:** Filters enable radio receivers to only "see" the desired signal while rejecting all other signals (assuming that the other signals have different frequency content).

- **DC power supplies:** Filters are used to eliminate undesired high frequencies (i.e., noise) that are present on AC input lines. Additionally, filters are used on a power supply's output to reduce ripple.
- **Audio electronics:** A crossover network is a network of filters used to channel low-frequency audio to woofers and mid-range frequencies to midrange speakers.
- **Analog-to-digital conversion:** Filters are placed in front of an ADC input to minimize aliasing.

1.5 Conclusion

In this chapter the basic theory of filters was introduced. Ideal filters, with a rectangular shape, indicating that the boundary between the passband and the stopband was abrupt and that the roll off slope was infinitely steep, would allow us to completely separate signals at different frequencies from one another. unfortunately, such an amplitude response curve is not physically realizable. We introduced approximations that will still meet our requirements for a given application. There are five types of filters are low-pass, high-pass, band-pass, and notch/band-reject, all-pass Filters, they serve a critical role in many common applications. Such applications include power supplies, audio electronics, and radio communication.

Chapter 2

Generalities on metamaterials

Chapter 2: Generalities on Metamaterials

2.1 Introduction

The concept of metamaterial is used along with filter to enhance those features. This material is an engineered material with some decent properties that are generally not found in nature.

Before entering into the project details, let us describe in this chapter some useful concept of metamaterials and their application in filter is given.

2.2 Metamaterials

Metamaterials (MTMs) are artificial materials engineered to provide properties which "may not be readily available in nature". These materials usually gain their properties from structure rather than composition, using the inclusion of small in homogeneities to enact effective macroscopic behavior. The metamaterials have entered into the main stream of electromagnetics. The essential property in metamaterials is their unusual and desired qualities that appear due to their particular design & structure. In particular composite media electromagnetic waves interact with the inclusions which produce electric and magnetic moments, which in turn affect the macroscopic effective permittivity and permeability of the bulk composite medium. Since metamaterials can be synthesized by embedding artificially fabricated inclusions in a specified host medium. This provides the designer with a large collection of independent parameters such as properties of host materials, size, shape, and compositions of inclusions. All these design parameters can play a major role in getting the final result. In these the shape of the inclusions is one that provides a new possibility for metamaterial processing [3].

2.3 Some properties of metamaterials

2.3.1 Reversal of Snell's law

In Metamaterials Refractive index in the Snell's law is negative. N. Engheta (2006) described that an incident wave faces negative refraction at the interface Ray bends in inside direction after refracting in to medium which is contrary to positive index medium

as shown in fig 2-1. Light is refracted in a contrary way as compared to the normal "right-handed material" [7].

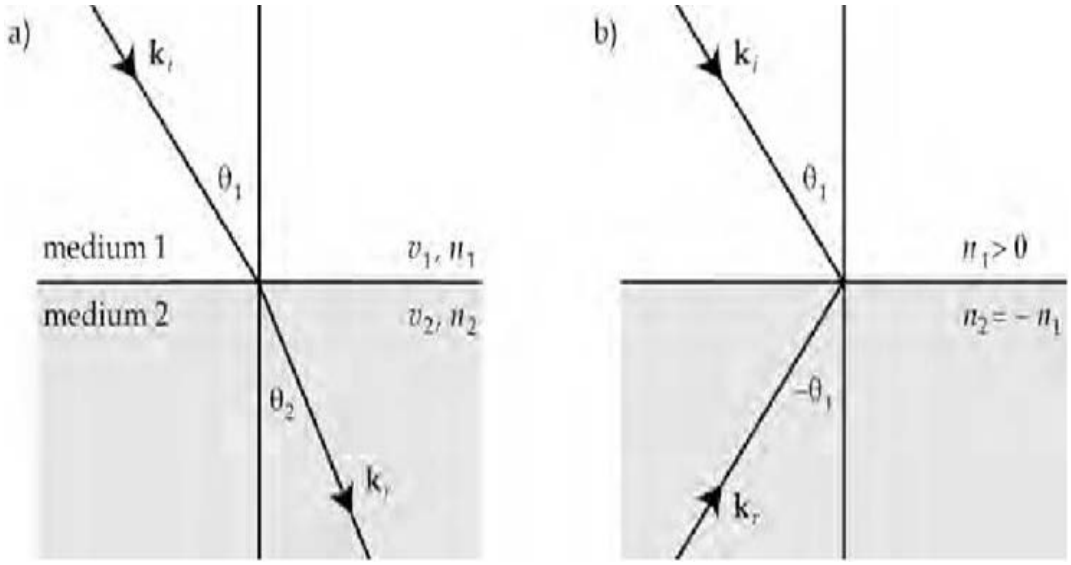

Figure 2-1 Snell's law illustration in (a)ordinary material and (b) metamaterials.

2.3.2 Reversal of Maxwell's equation

Maxwell's equations are one of the most elegant and concise mathematical tools to describe the fundamentals of electromagnetic field. According to Maxwell's equations the negative permittivity and negative permeability are caused by the antiparallel phase and group velocities or LH wave. The Maxwell's equations analysis mentioned in the following Equations and can be written as [11]:

$$\nabla \times \vec{E} = -jw\mu\vec{H} - \overrightarrow{M_s} \qquad (2-1)$$

$$\nabla \times \vec{H} = jw\mu\vec{E} + \overrightarrow{J_s} \qquad (2-2)$$

$$\nabla . \vec{D} = \rho_e \qquad (2-3)$$

$$\nabla . \vec{B} = \rho_m \qquad (2-4)$$

with

$$\vec{D} = \varepsilon\overrightarrow{E} \qquad (2-5)$$

$$\vec{B} = \mu\vec{H} \qquad (2-6)$$

Where $\overrightarrow{J_s}$ is the electric current density, $\overrightarrow{M_s}$ is the magnetic current density , ρ_e is the electric charge density, and ρ_m magnetic charge density.

The time dependence of convention is explicitly represented by the factor for the

harmonic fields. In the ideal case, which means loss-less medium, the magnetic and electric current densities will vanish such that,

$$\overrightarrow{M_s} = \overrightarrow{J_s} = 0 \qquad (2-7)$$

After introducing the plane wave conception into the first of two Maxwell's equations, the mathematic expressions of $\vec{E}$, $\overrightarrow{H}$ *and* $\vec{\beta}$ and (wave vector) is obtained. The Poynting vector represents the direction of transfer of energy flux density of an electromagnetic field. It can be written as:

$$\vec{S} = \vec{E} \times \vec{H} \qquad (2-8)$$

For right-handed (RH) materials, $\varepsilon, \mu > 0$ for left-handed (LH) materials, $\varepsilon, \mu < 0$ The spatial relations of these parameters for RH and LH are shown is Fig 2-2(a) and Fig 2-2(b), respectively

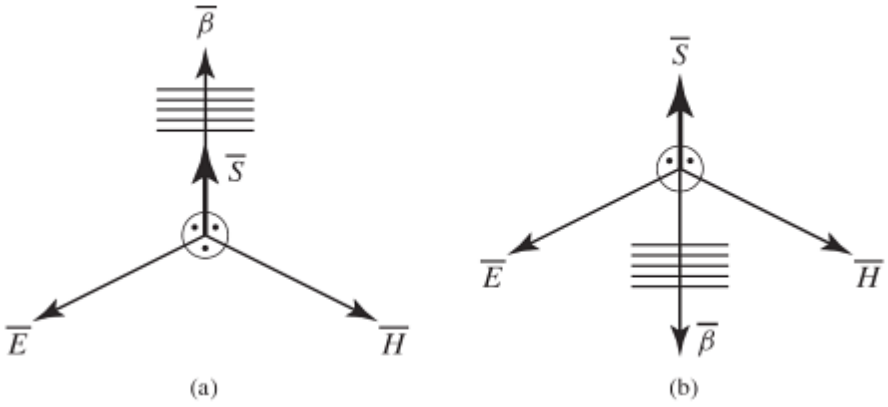

Figure 2-2 The spatial relations of E, β, and H for (a)RH and (b)LH.

The main difference between Fig 2-3(a) and Fig 2-3(b) is the directions of the Poynting vector and the wave vector are parallel or antiparallel for the RH medium and the LH medium, respectively [11]

In the right hand medium

$$\overrightarrow{\beta} \times \vec{E} = +\omega\mu\vec{H} \qquad (2-9)$$

$$\vec{\beta} \times \vec{H} = -\omega\varepsilon\vec{E} \qquad (2-10)$$

In the left hand medium

$$\vec{\beta} \times \vec{E} = -\omega|\mu|\vec{H} \qquad (2-11)$$

$$\vec{\beta} \times \vec{H} = +\omega|\varepsilon|\vec{E} \qquad (2-12)$$

2.4 Material classification

The response of a system to the presence of Electromagnetic field is determined by the properties of the materials involved. These properties are described by defining the macroscopic parameters permittivity ε and permeability μ of these materials. By using permittivity ε and permeability μ the classification of metamaterials as follows, the medium classification can be graphically illustrated as shown in fig (2.3) [3].

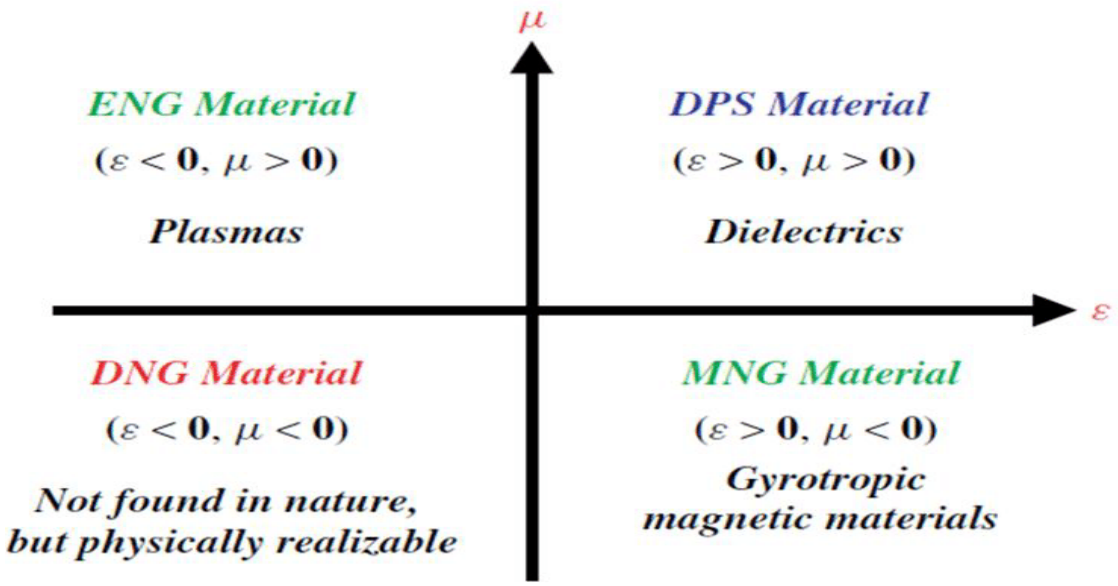

Figure 2-3 Classification of materials in function of the sign of their permittivity ε and permeability μ.

A medium with both permittivity & permeability greater than zero ($\varepsilon > 0$, $\mu > 0$) are called as double positive (DPS) medium. Most occurring media (e.g. dielectrics) fall under this designation.

A medium with permittivity less than zero & permeability greater than zero ($\varepsilon<0$, $\mu > 0$) are called as Epsilon negative (ENG) medium. In certain frequency regimes many plasmas exhibit these characteristics.

A medium with both permittivity greater than zero & permeability less than zero ($\varepsilon > 0$, $\mu < 0$) are called as Mu negative (MNG) medium. In certain frequency ranges some gyrotropic material exhibits this characteristic.

A medium with both permittivity & permeability less than zero ($\varepsilon<0$, $\mu<0$) represents Metamaterial, also called left-handed material or double negative material (DNG). It follows the left-handed rule because propagation of wave takes place in backward direction in this medium. Due to negative μ and negative ε the refractive index of the medium is calculated to be negative. Thus, also termed as NIM (negative index material).

Fig. 2-3 and the expression (2-7) give a distinct explanation, for how negative permittivity and negative permeability lead to antiparallel phase and group velocities.

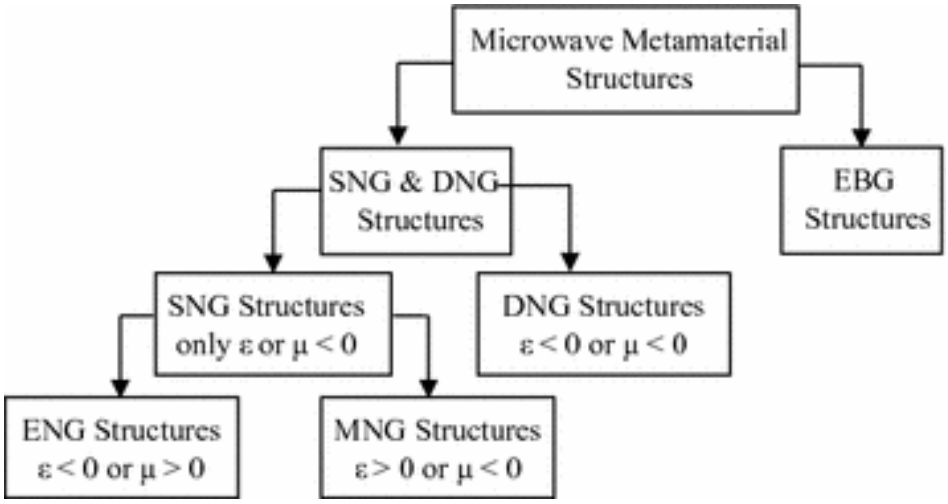

Figure 2-4 Microwave metamaterial tree.

2.4.1 Epsilon negative (ENG) Metamaterial

The first and the most-known ENG-material for microwave applications are thin metal wires. The structure consists of a square matrix of infinitely long parallel thin metal wires, embedded in a dielectric medium. Propagation of electro- magnetic waves in such a structure is similar to propagation in plasma. Permittivity of composite material is negative at frequency $\omega < \omega p$, where ωp is the plasma frequency of the structure. Its value depends on the radius and placement period of wires, therefore, plasma frequency of such structure is controlled. Effective permittivity can be written as[15]

$$\varepsilon_{eff} = 1 - \frac{\omega_p^2}{\omega[\omega - i(\omega_p^2 a^2 \varepsilon_0)/\sigma\pi r^2]} \qquad (2-13)\ [15]$$

where r is the radius of individual wire, a is the period between the wires with r << a, σ is electrical conductivity.

Another example of wire ENG-structures is three-dimensional structure proposed in [16]. A lattice of infinitely long connected wires forms triplet element (Fig. 2-5). Using effective medium approach, the attenuation and phase constants of modes that propagating in the triple wire medium have been calculated both below and above the plasma frequency. It has been discovered that the wave propagates below the plasma frequency along all the spatial directions with the same attenuation coefficient. So, the triple structure is characterized by the isotropy relative to the direction of electromagnetic waves.

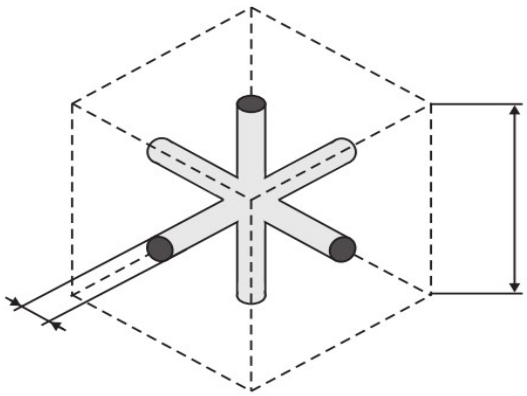

Figure 2-5 Triple wire isotropic structure.

2.4.2 Mu negative (MNG) Metamaterial

The first and the most widely-used MNG-structure is split-ring resonator (SRR) [8]. SRRs can be both round and square geometrically, are characterized as high-conductive resonant structure, in which the capacitance between the two rings balances the inductance. A time-varying magnetic field applied perpendicular to the rings surface induces currents that produce the secondary magnetic field. In dependence on the resonant properties of the structure, it can either oppose or enhance the incident field, thus resulting in positive or negative μ_{eff}[15]. A few unit cells geometries of MNG-material based on the SRR are shown on Fig. 2-6 [3].

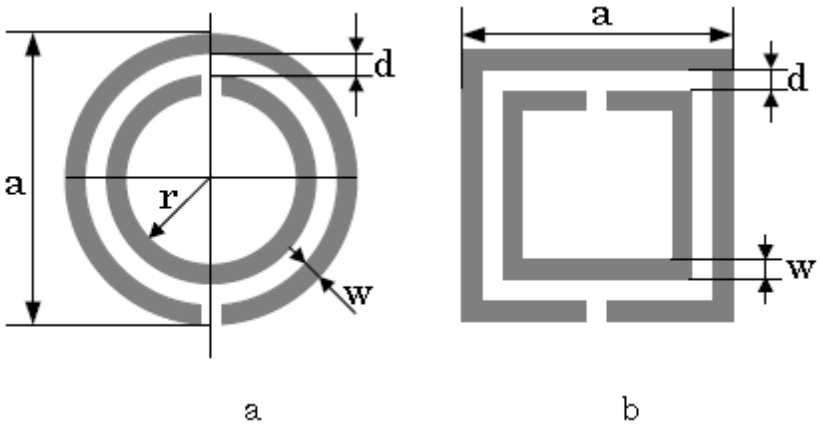

Figure 2-6 Basic SRR (a)circular, and (b) rectangular

$$\mu_{eff} = 1 - \frac{\pi r^2/a}{1+\frac{2\sigma i}{\omega r \mu_0}+\frac{3d}{\pi^2 \mu_0 \omega^2 \varepsilon_0 \varepsilon r^3}} \qquad (2-14)[15]$$

where a is the unit cell length, d is the interval between the rings, r is the radius of the inner ring, and σ is the electrical conductance.

Main disadvantages of the first metamaterials based on circular or rectangular SRRs are narrow frequency band where $\mu_{eff} > 0$ and high levels of electromagnetic losses. Moreover, SRR is actually anisotropic structure. If the vector of magnetic field of the incident plane wave is perpendicular to the SRR, as a result we will observe the negative permeability. However, if the magnetic field vector is parallel to the SRR, it cannot influent on the induced currents and does not affect the μ_{eff}, so the first SRR is characterized as one-dimensional unit cell [3]. In order to overcome such anisotropy a few ways have been presented

The simplest method is to placing the same planar SRRs in three orthogonal space directions and thus forming a group matrix of unit cells and achieving an anisotropy [23]. Alternative topologies of the structure have been proposed as well. Unit cell variations of the rectangular SRR are shown in Fig 2-7. In whole, electrophysical properties of various modifications of microwave SRR are sufficiently studied [23-30]. Numerical study performed using the finite integration technique (FIT) and transfer matrix method (TMM) on the Microwave Studio software has shown that the most promising and potentially successful structures for microwave technique are SRRs from the second row

on Fig. It has been determined that more symmetrical structure (for instance, on Figure &-7, c) than the original (Fig. 2-7, a) allows to distribute the capacity in the rings equivalently between the two gaps. It reduces the cross-polarization effects that lead to electromagnetic losses in the overall system. The summarizing of theoretical and experimental studies of ring resonators is the broadside-coupled SRR (Fig. 2-7, h), which is constituted of two identical rectangular or round micro resonators located on both sides of the dielectric substrate with the gaps on opposite sides. Such approach to forming unit cells leads to the isotropy of obtained composite structure as well reduces its electrical size in the resulting DNG-material at the operating frequency. Consequently, the further material description as a homogeneous media is simplified and thus makes it using in practical microwave applications more convenient.

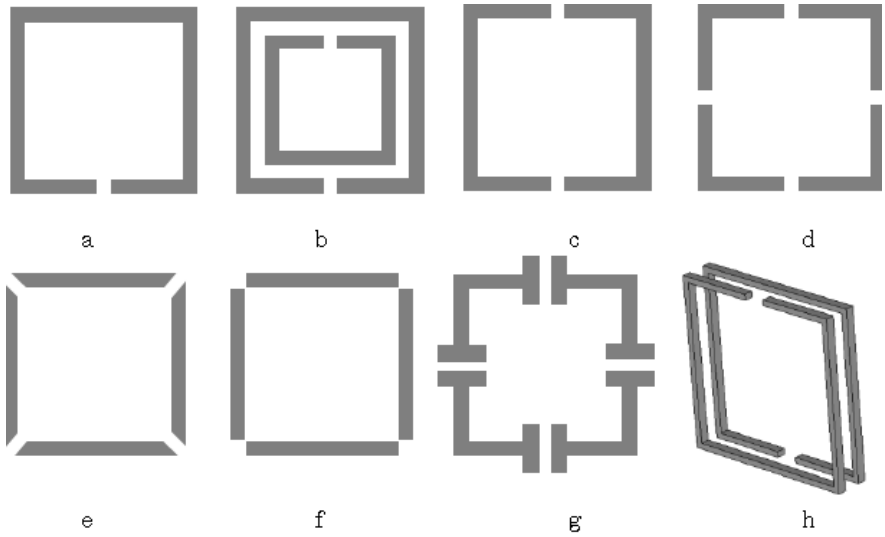

Figure 2-7 The Basic modifications of rectangular SRRs

With applying the Babine principle to convenient SRRs the complementary structures (Fig. 2-8) abbreviated CSRRs were engineered and manufactured [31]. CSRR unit cells are the holes of corresponding form in the metal surface. Such a structures belong to the ENG-materials and negative ε_{eff} is obtained in a narrow frequency range near the resonance.

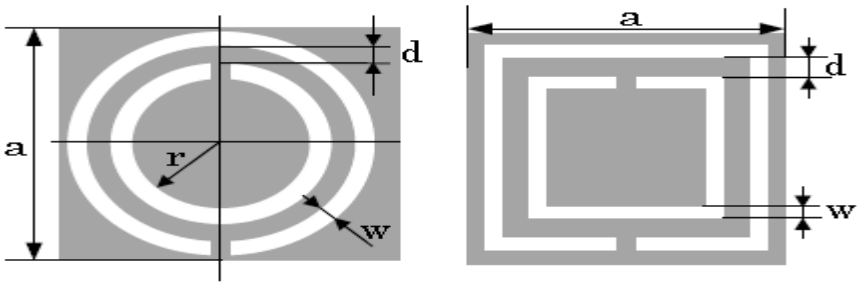

Figure 2-8 Unit cells of ENG-materials based on complementary split ring resonators: a) round, b) square Grey - thin metal surface

According to the classification scheme (Fig. 2-4) the MNG structures class includes helical structures and S-shaped resonators as well (Fig. 2-9). They have been also constructed in order to improve the characteristics of original split ring resonators. The main advantages of its unit cells compared to SRRs is compactness, easy manufacture with obtaining the homogeneous DNG-material with the same resonant frequency.

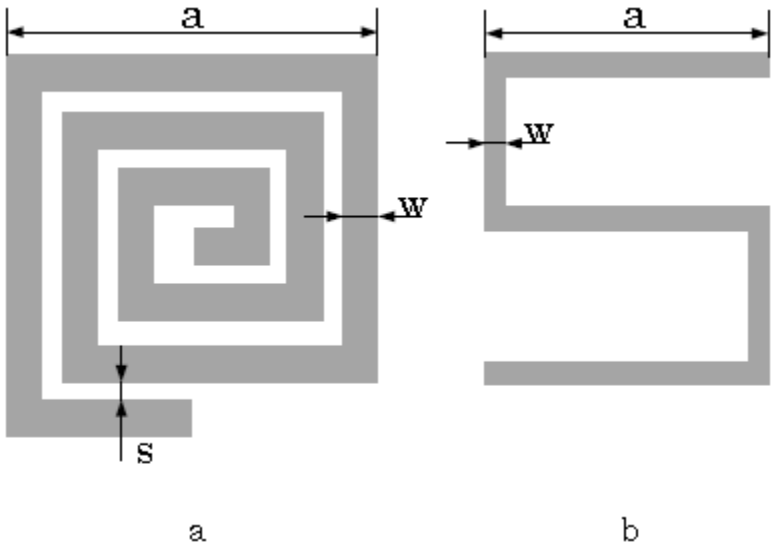

Figure 2-9 Units cells of alternative MNG-structures a) spiral resonator, b) S-shaped resonator

2.4.3 Double negative (DNG) Metamaterial

We divided the most prevalent approaches to design metamaterials with negative refractive index into three main classes: thin wires & SRR, transmission lines and mushroom structure. The pioneer structure, is the combination of split ring resonators and thin metal wires. the schematic is represented on Figure (2-10).

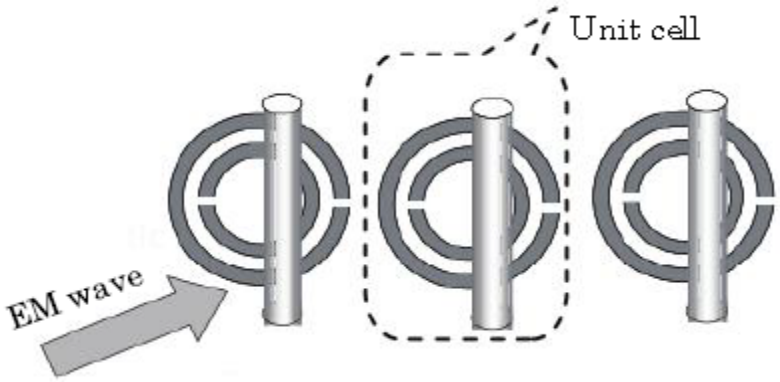

Figure 2-10 The array of unit cells for ring and wire structures

Negative values of effective permittivity and permeability of corresponding composite structure have been confirmed by experiments in the waveguide chamber [17]. Fundamental properties of structure also have been tested by numerical simulations [18]. Because of resonance properties of the unit cell, an anomalous electromagnetic radiation and thus negative index of refraction have been observed in a very narrow frequency range, which restricts the applicability of such structures. One can partially expand the frequency range by using other planar MNG-structures in place of SRRs, such as improved modification of split rings (Fig. 2-7), S-shaped and spiral resonators and met solenoids for several applications.

An alternative approach to forming DNG- metamaterial is transmission line structures that are extensively used in microwave technique. In contrast to thin ring and SRRs structure, transmission lines are non-resonant and mostly planar. The most convenient approach to describe unit cells and total systems based on metamaterial transmission lines is the method of equivalent circuits. It is based on represent metamaterial structures coupled to planar transmission lines of different types by lumped- element circuit models. As well, it allows determining the main circuit

parameters for these models.

As known from transmission line theory, the volt- age and the current in transmission line and its components are in agreement with components of the electromagnetic field. For isotropic homogeneous medium the impedance and admittance can be written as:

$$Z = i\omega\mu \qquad (2-15)$$

$$Y = i\omega\varepsilon \qquad (2-16)$$

Whereas those variables for left-handed transmission line are defined as:

$$Z' = \frac{1}{i\omega c} \qquad (2-17)$$

$$Y' = 1/i\omega l \qquad (2-18)$$

So, such transmission line is similar to the dual distributed network with a sequence of parallel capacitors and inductance. Actually, it can be characterized as high pass filter that supports the propagation of backward waves. A unit cell of transmission line DNG material with parasitic series inductance and shunt capacitance is shown on Fig. 2-11.

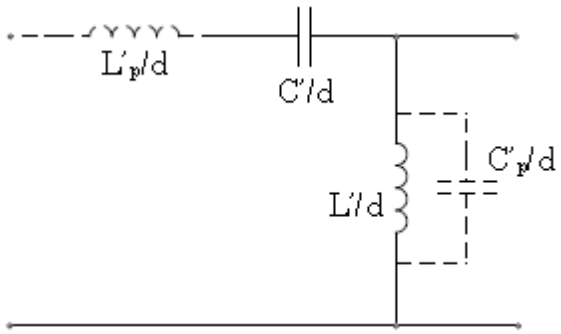

Figure 2- 11 An equivalent circuit for the transmission line unit cell. L'p and C'p are accordingly parasitic inductances

A wave propagation through the metamaterial transmission line is described by the telegrapher's equation. DNG-properties of obtained composite structure are observed at frequencies below the cutoff frequency. In turn, structure behaves like a conventional material above the cutoff frequency, hence it have been defined as CRLH-structure (composite right/left-handed structure) [27]. Planar metamaterial transmission lines are

typically implemented as combination of SRRs and complementary structures coupled by microstrip technology or by embedding it to the structure of planar waveguide. In order to obtaining larger bandwidths and lower losses, the lumped circuit elements can be added in unit cells.

The third mushroom structure (Fig. 2-12) termed in such manner because of unit cells' shape, which resemble a mushroom caps and stems. It is similar to previous structure and relates to the CRLH-structures as well

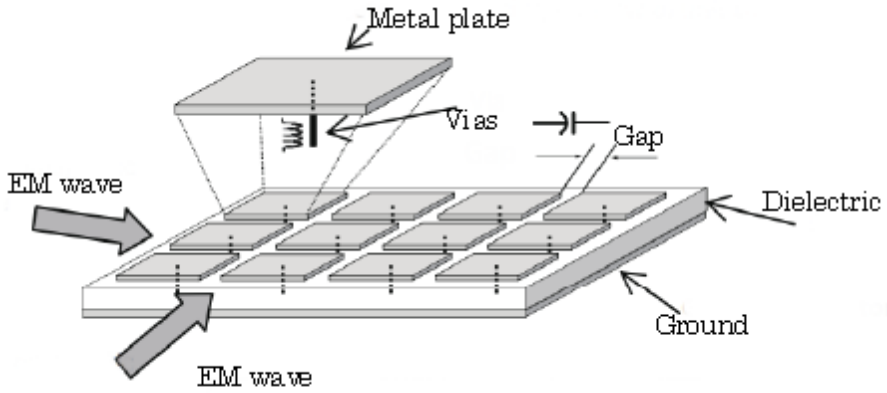

Figure 2-12 Mushroom metamaterial structure

In order to form the metamaterial unit cells a metal patches are periodically arranged in a matrix over the lower conductive layer. The gaps between the patches form capacitances and the vias form inductances.

Mushroom structure has properties of both right and left-handed material depending on frequency as the previous one; hence it is a CRLH-structure as well. Such a structure has features, which are suitable for low-and-high-pass filter implementation for frequency range around those in which the structure has left-handed properties [26]. Different types of MNG materials can be used as metal cells in mushroom structure: SRRs and derived configurations, Ω-shaped and chiral structures. The successful example is mushroom metal-dielectric structure with PIN diodes placed along the direction of the vias. Such structure with multi-diode switch allow minimizing the undesired transmission for a certain incident angle [30].

The mushroom structure with diodes can be applied in dual-band subwavelength imaging where the operation frequency can be controlled by changing the states of diodes.

2.5 Applications

- Microwave filters
- Metamaterials are used to improve performances of antenna system.
- Superlens uses metamaterials to go beyond the diffraction limit.
- Metamaterials provide tools to significantly enhance the sensitivity and resolution of sensors

2.6 Limitations

The metamaterials present some limitations such as

- Work for limited range of wavelength.
- Difficult to produce in large quantities.
- Shape cannot be change during operation.
- Lossy.

2.7 Conclusion

In this part we saw the main electromagnetic properties of metamaterials such: the reversal of Snell's law, refractive index, and Maxwell equations. We also discussed the main types of metamaterials which are ENG, MNG, and DNG.

Chapter 3

Design of dual-band bandpass filter

Chapter 3: Design of dual band bandpass filter

3.1 Introduction:

In this chapter, a dual-band BPF, operating at two central frequencies of 3.5 GHz and 5.8GHz, based on metamaterial triangular split ring cell will be developed. It will be performed in FR4 substrate with relative dielectric constant of 4.3, thickness 1.63 mm and a dialectic loss tangent 0.017. The design and results will be conducted using CST microwave studio.

3.2 Design steps procedure:

Before we go to our design procedure an outline of the dimensions used in the design is shown in figure (3-1)

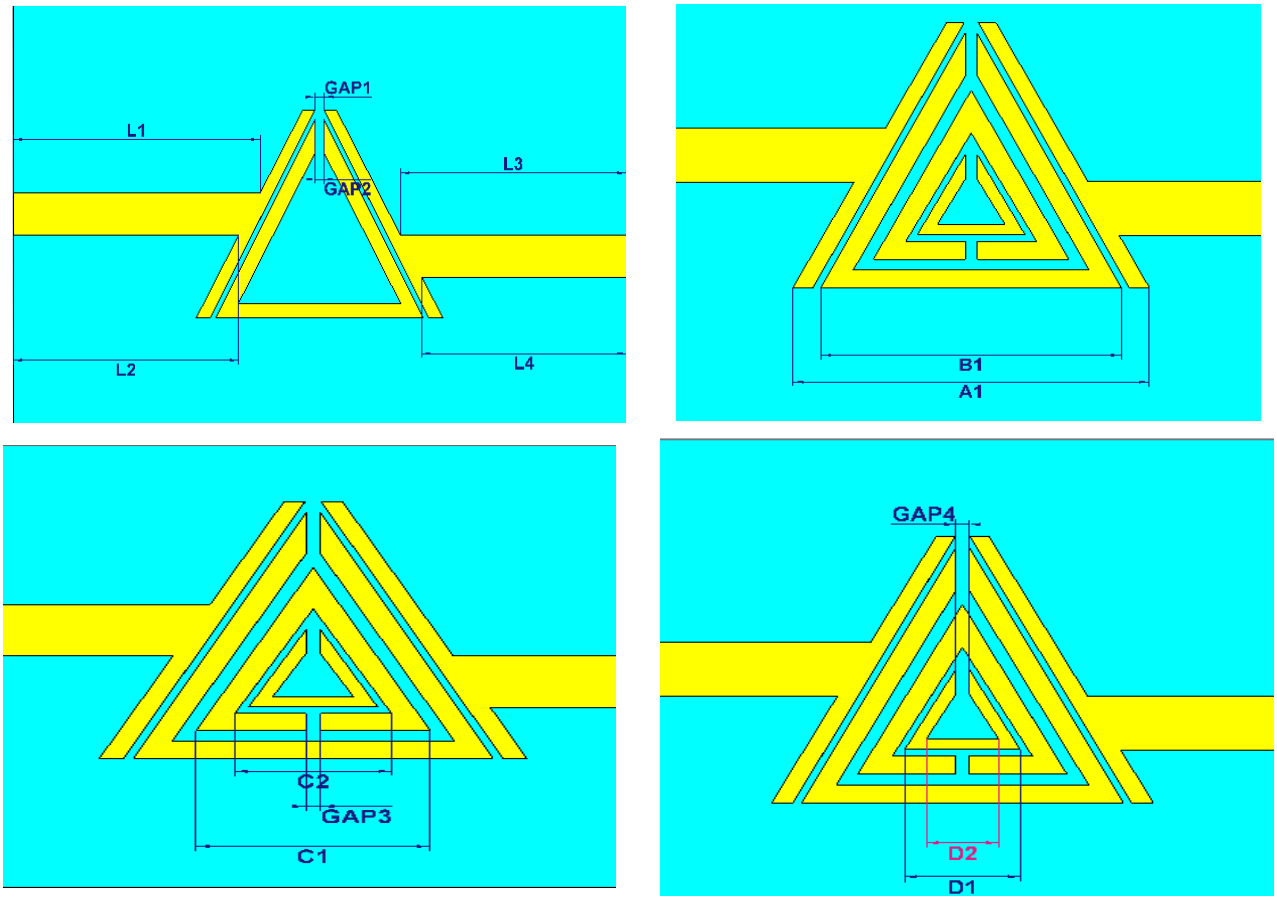

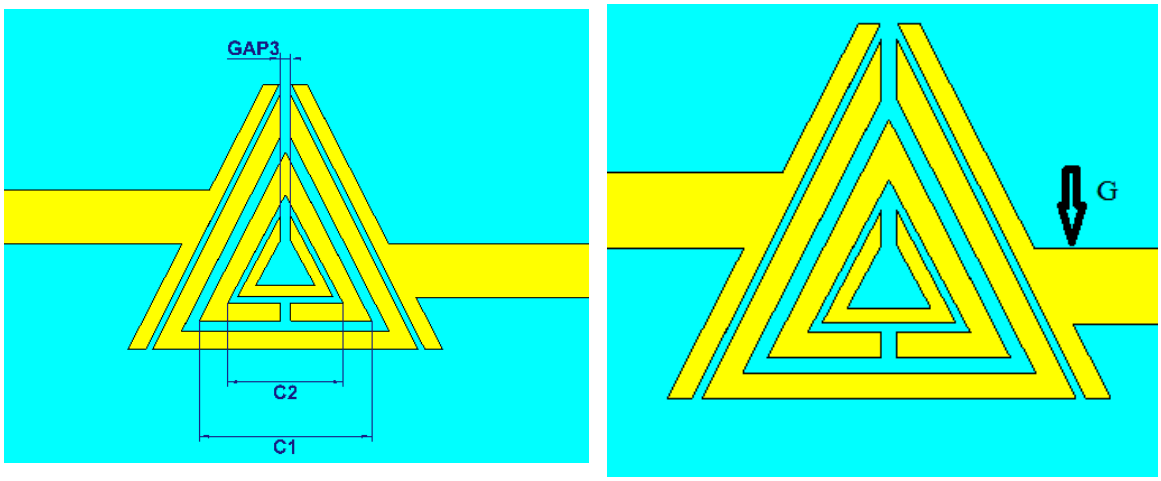

Figure 3. 1 Outline of the dimensions used

First, the width of the microstrip line (Wl) and thickness of substrate (Ts) are tuned using the " calculate analytical line impedance " tool in macros>calculate menu. The material that was used for the line is copper. They are tuned to reach a characteristic impedance of 75 ohms. The value of 75 ohms was chosen to get appropriate smaller microstrip width .For a FR-4 substrate of $\varepsilon_r = 4.3$, the results were Wl =1.51mm , h =1.63 mm (figure 3-2). A copper ground plane of thickness 0.035 mm is attached to the substrate. We chose the length of the line to be 22 mm because it fits the following steps. the result is shown in figure (3-3) and the S parameters are shown in figure (3-4).

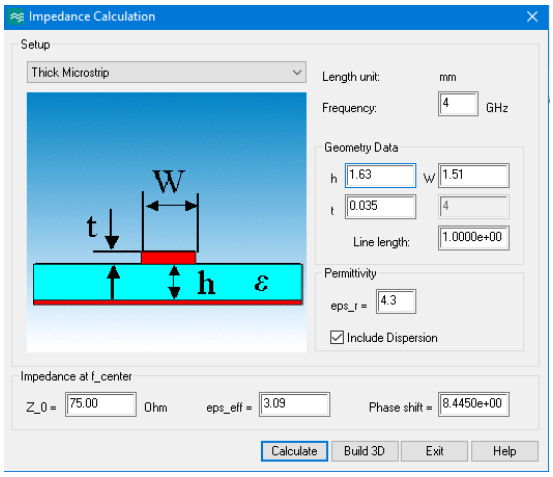

Figure 3. 2 Impedance calculation using CST software

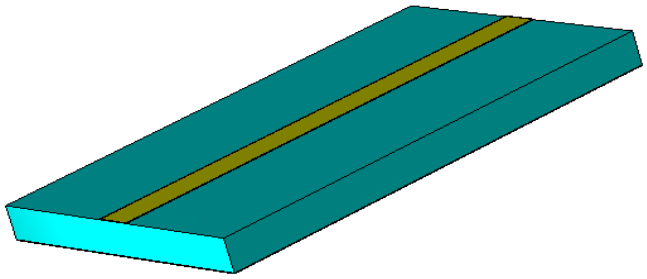

-

Figure 3. 3 3D model of the Microstrip line

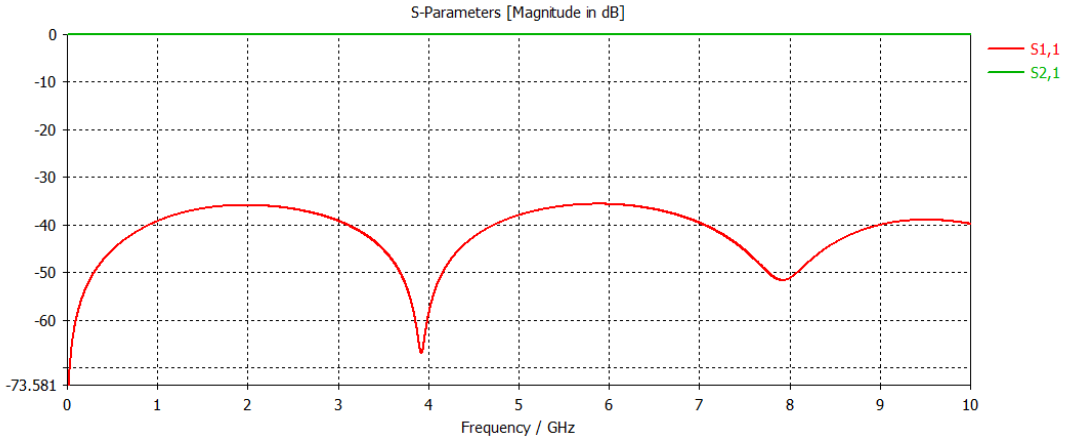

Figure 3. 4 Simulated S-parameters for the Microstrip line

For the second step we add the first triangular split ring resonator with a gap of 0.35 mm at the top angle as shown in figure 3-5, this step creates the first passband as shown in figure 3-6.

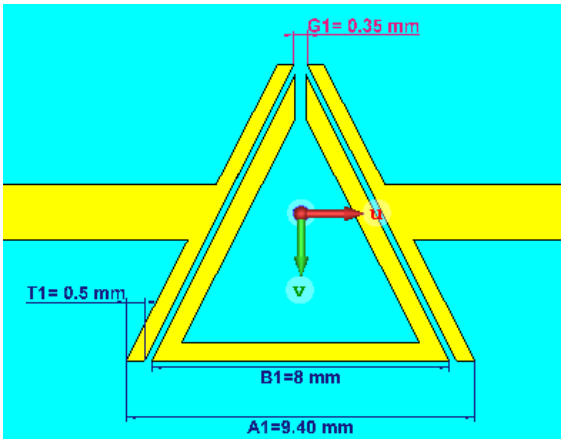

Figure 3. 5 3D model for the filter with one triangular SRR

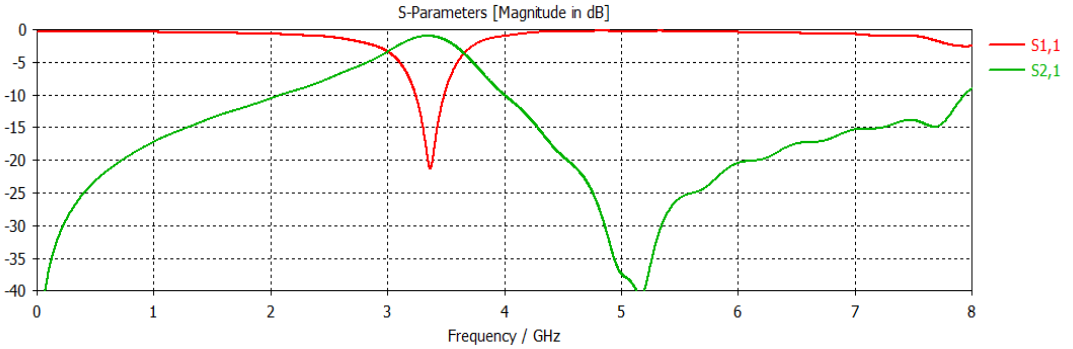

Figure 3. 6 simulated S parameters for the design with one triangular SRR

Then, in order to achieve the second passband at a frequency higher than the previous one we add a smaller triangular split ring resonator with a gap at the base as shown in figure 3-7.the simulated S parameters are shown in figure 3-8

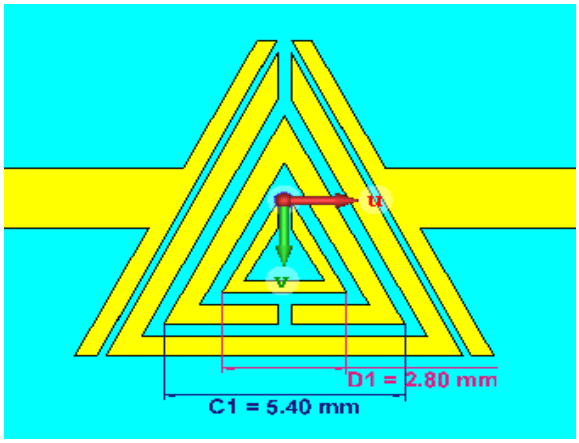

Figure 3. 7 3D model of the filter with two triangular SRRs

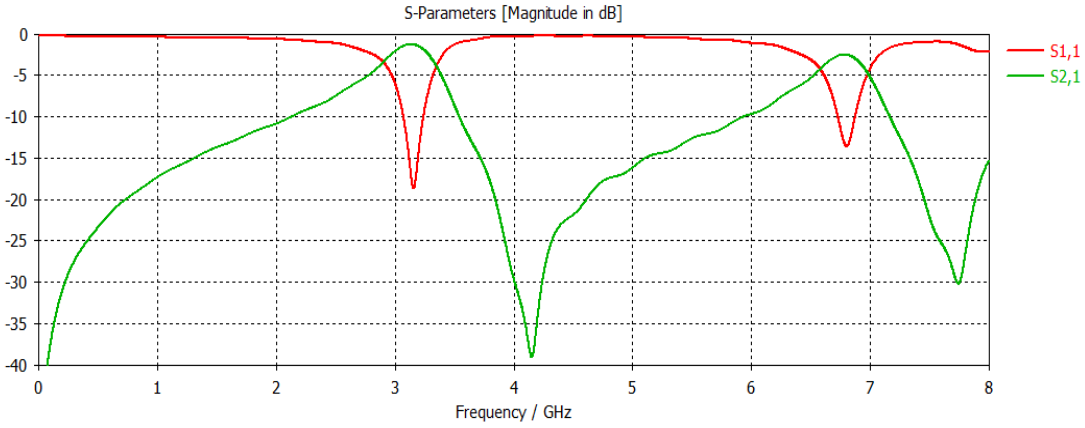

Figure 3. 8 Simulated S-parameter for the filter with two SRRs

The next procedure we add a link between the two smallest triangular rings to increase the attenuation in return loss at the second frequency band as shown in figure 3-8.the corresponding S parameters are shown figure (3-9).

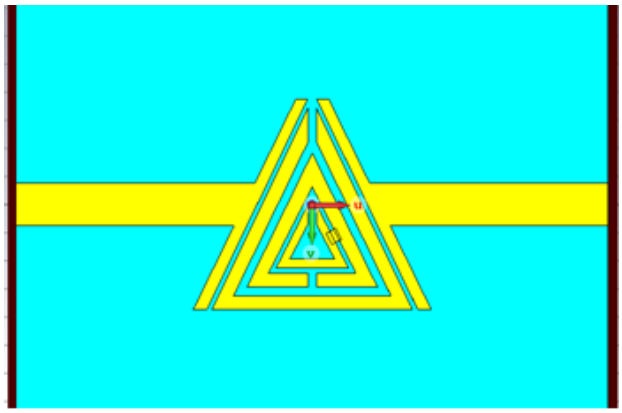

Figure 3. 9 3D model of the design with two SRRs and a link

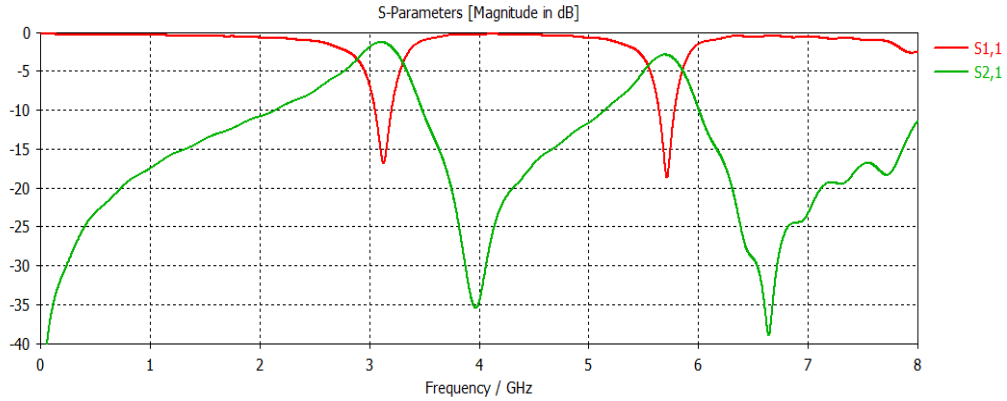

Figure 3. 10 Simulated S parameters of the design with two SRRs and a link

As Final procedure, we shift the position of the right part of the microstrip by a value G = 1.5 mm in order to increase the attenuation in the reflection coefficient S11 at the first frequency band:

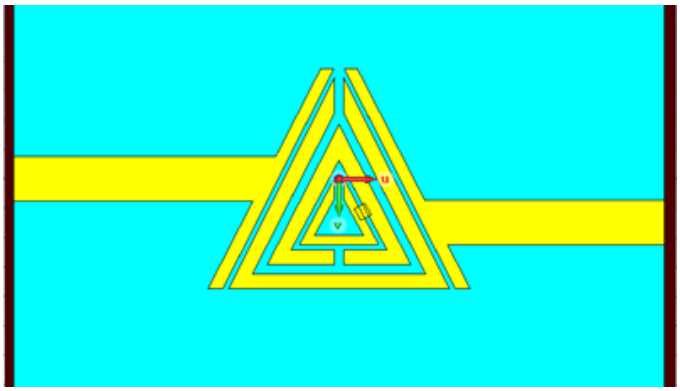

Figure 3. 11 3D model of the design after the shift of the microstrip

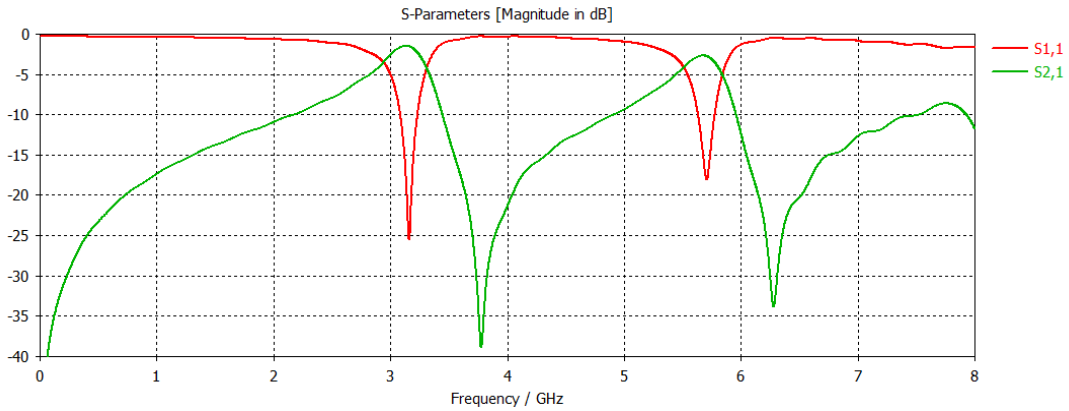

Figure 3. 12 Simulated S parameters of the design after the shift of the microstrip

3.2.1: Effect of changing dimensions on simulated S parameters:

After a lot of simulation the dimension changes that yield the most significant changes in performance are shown below :

3.2.1.1 The shift of the microstrip (G):

As shown in the steps of realization in section 3-2 the microstrip in the right part of the filter is shifted in order to get more attenuation in S11 at the first shown

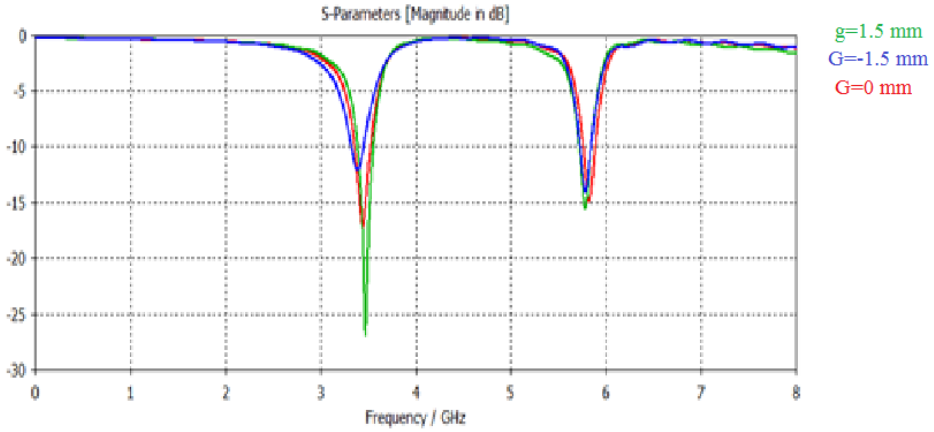

Figure 3. 13 effect of varying the shift G on S11

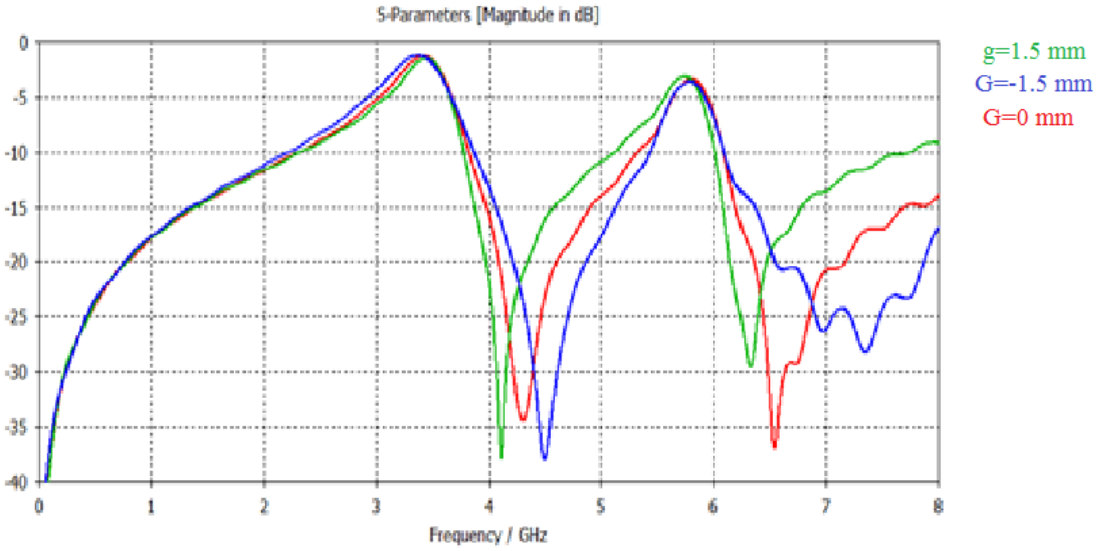

Figure 3. 14 effect of varying the shift G on S21

It is remarked that as the shift G is increased from -1.5 (the minus means the opposite direction) to 1.5 the attenuation in S11 is significantly increased from -10dB to -25 dB, as for S21 no significant change is observed.

3.2.1.2 The Variation of G4:

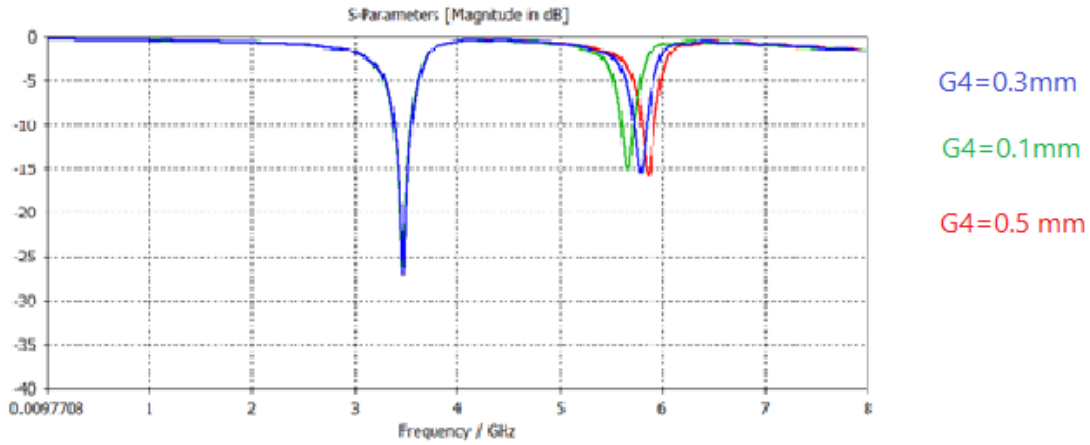

Figure 3. 15 effect of varying G4 on S11

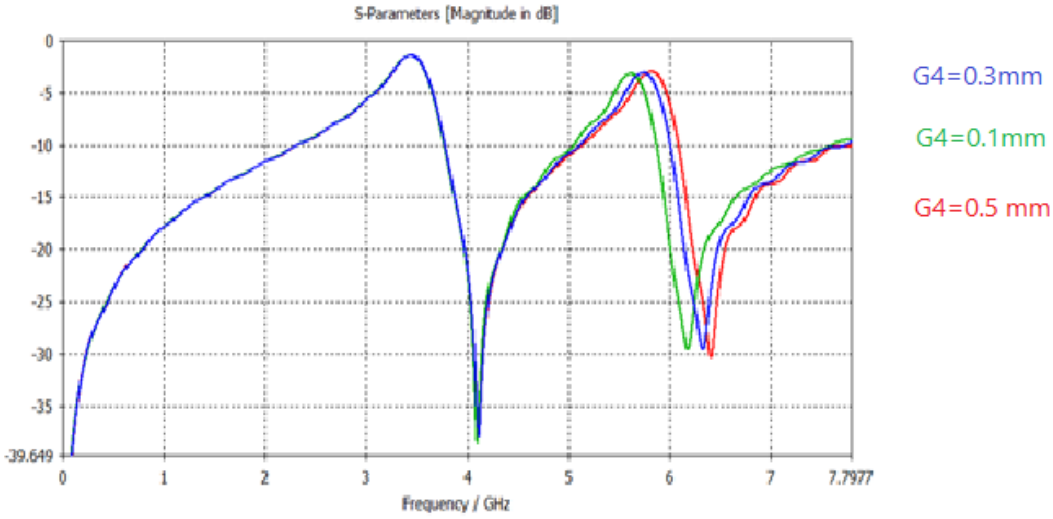

Figure 3. 16 effect of varying G4 on S21

As we change the gap G4 in the inner SRR we remark a shift in the higher central of the filter as shown in figure 3-14 and 3-15

3.2.1.3 The Variation of T_1:

The results of changing T_1 are shown in figure 3-16 and 3-17

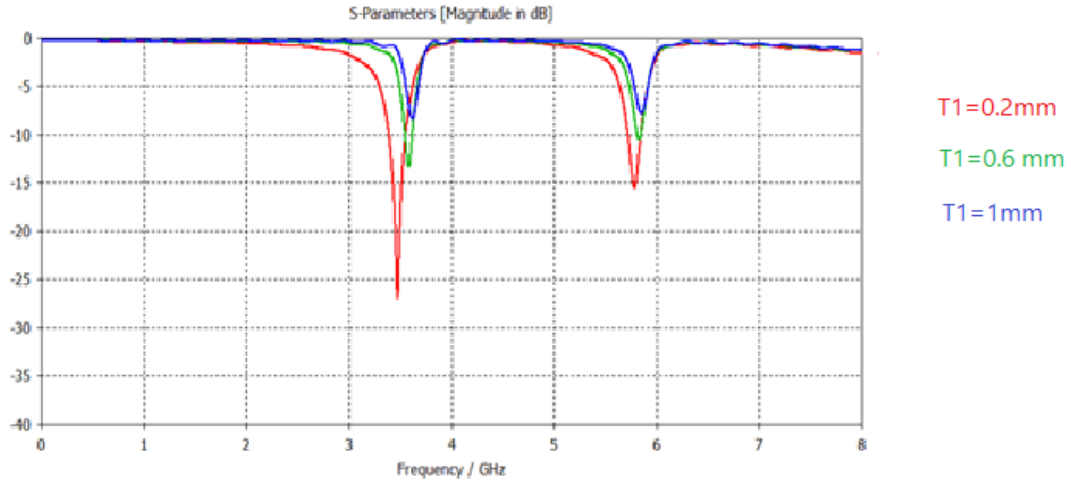

Figure 3. 17 Effect of changing T_1 on S11

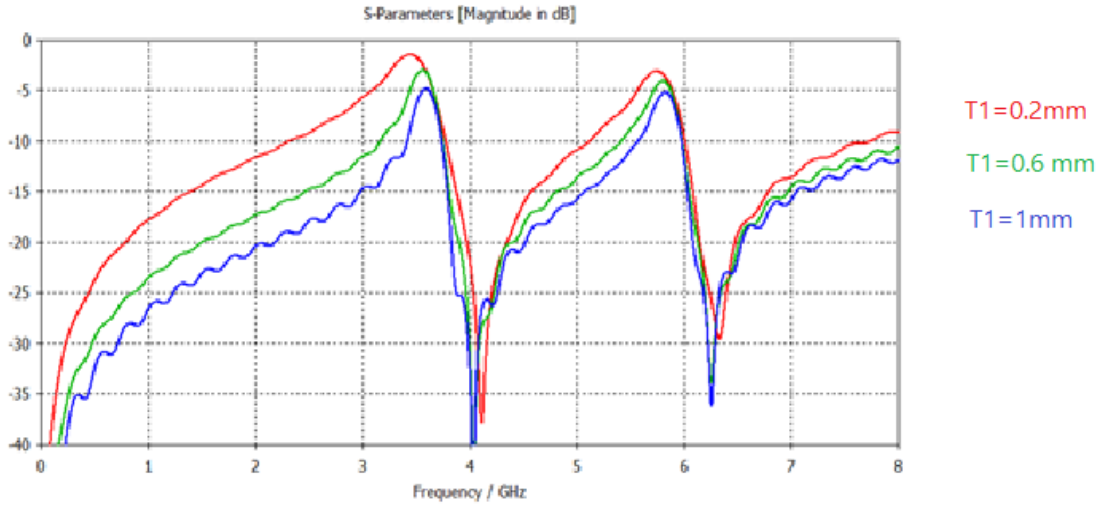

Figure 3. 18 Effect of changing T_1

As the dimension T_1 is increased from 0.2 mm to 1 mm we remark that the attenuation of S11 at the frequencies of interest is decreased, as for S21 the graphs falls far below the -3db line causing less transmission in the pass band, we also remark a decrease in the -20db rejection band.

3.2.1.4 The Variation of B1:

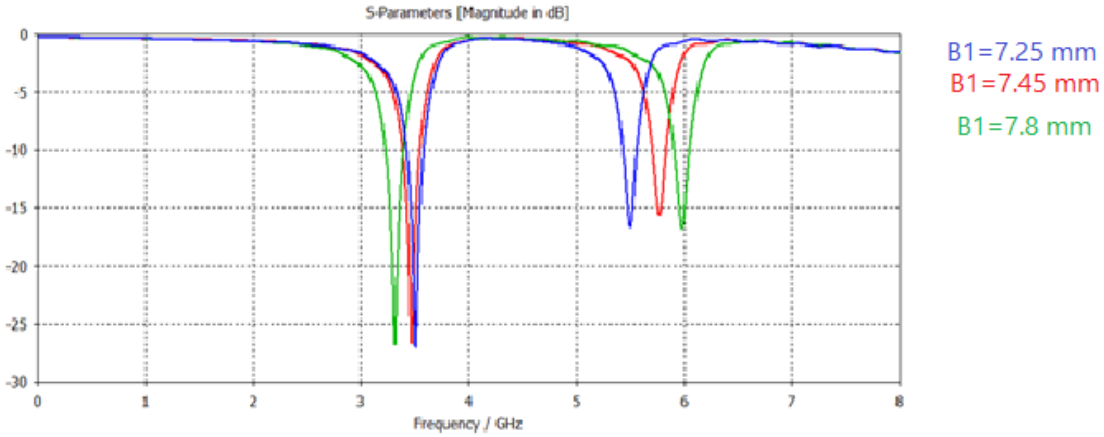

Figure 3. 19 effect of varying B1 on S11

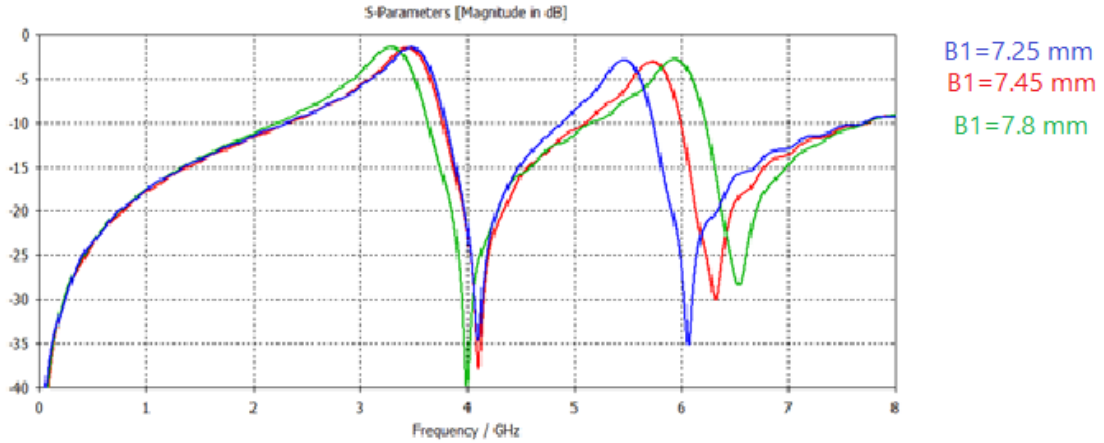

Figure 3. 20 Effect of varying B1 on S21

3.2.1.5 The Variation of p:

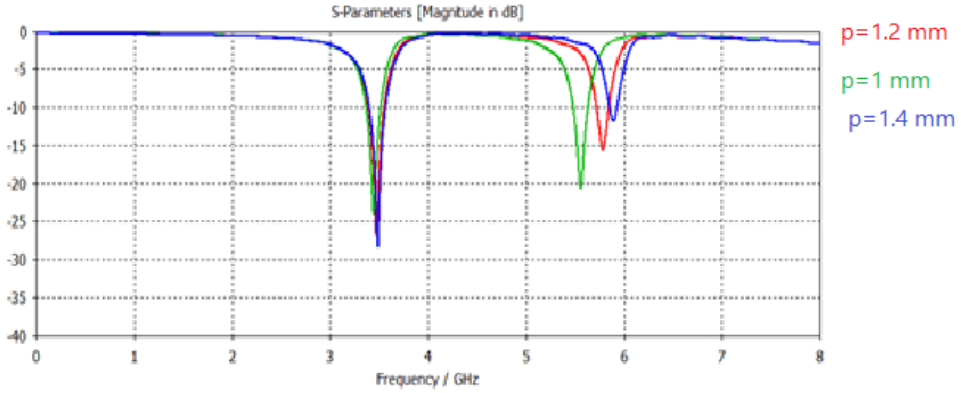

Figure 3. 21 effect of variation of p on S11 p = 1.2 (red), p = 1(green), p=1.4 (blue)

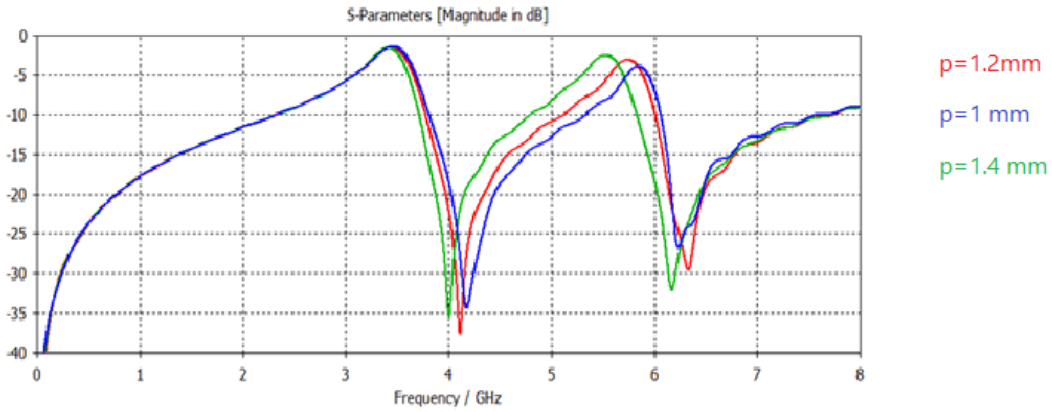

Figure 3. 22 effect of variation of p on S21

3.3 Final design and its performance

we attach the parts using Boolean addition tool in the simulator to get the final design shown in figure 3-12. The results of the filter show that it has two narrow passbands centered at 3.45 GHz and 5.79 GHz which are the frequency in which the WiMAX communication systems operates according to IEEE standard 802.16d. So, this filter can be useful to eliminate interferences from mobile networks such as GSM, 3G and LTE.

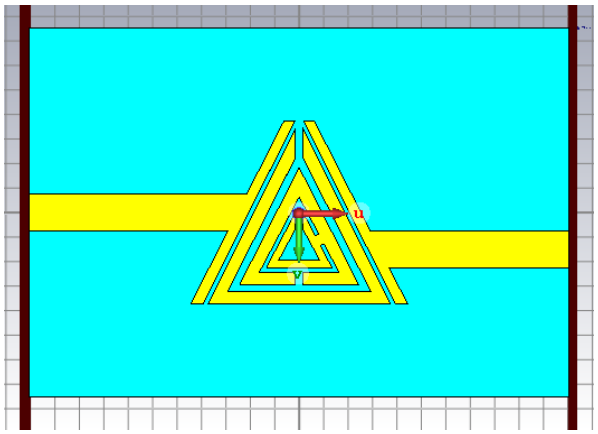

Figure 3. 23 3D model of the final design

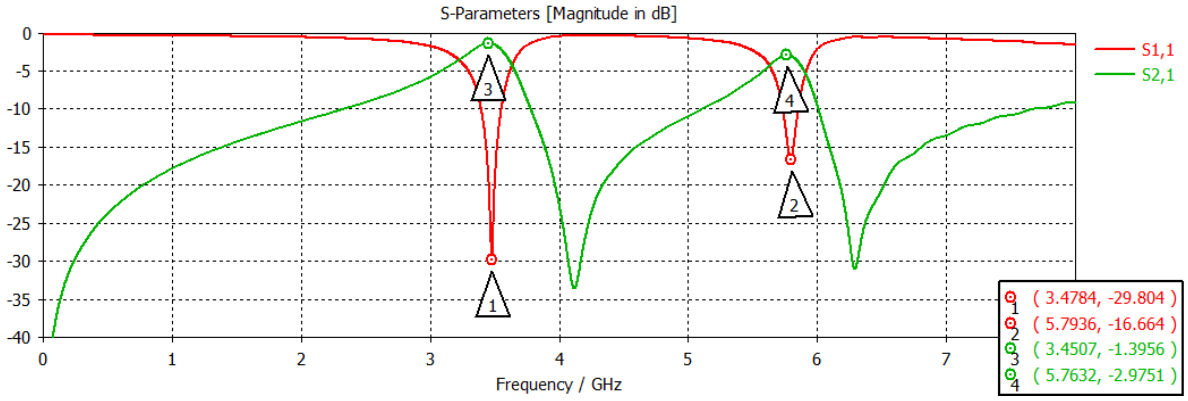

Figure 3. 24 Simulated S parameters for the final design

3.3.1 Final design dimensions:

The dimensions of the final design are discussed in figure 3-14(a) and (b), and table 3-1

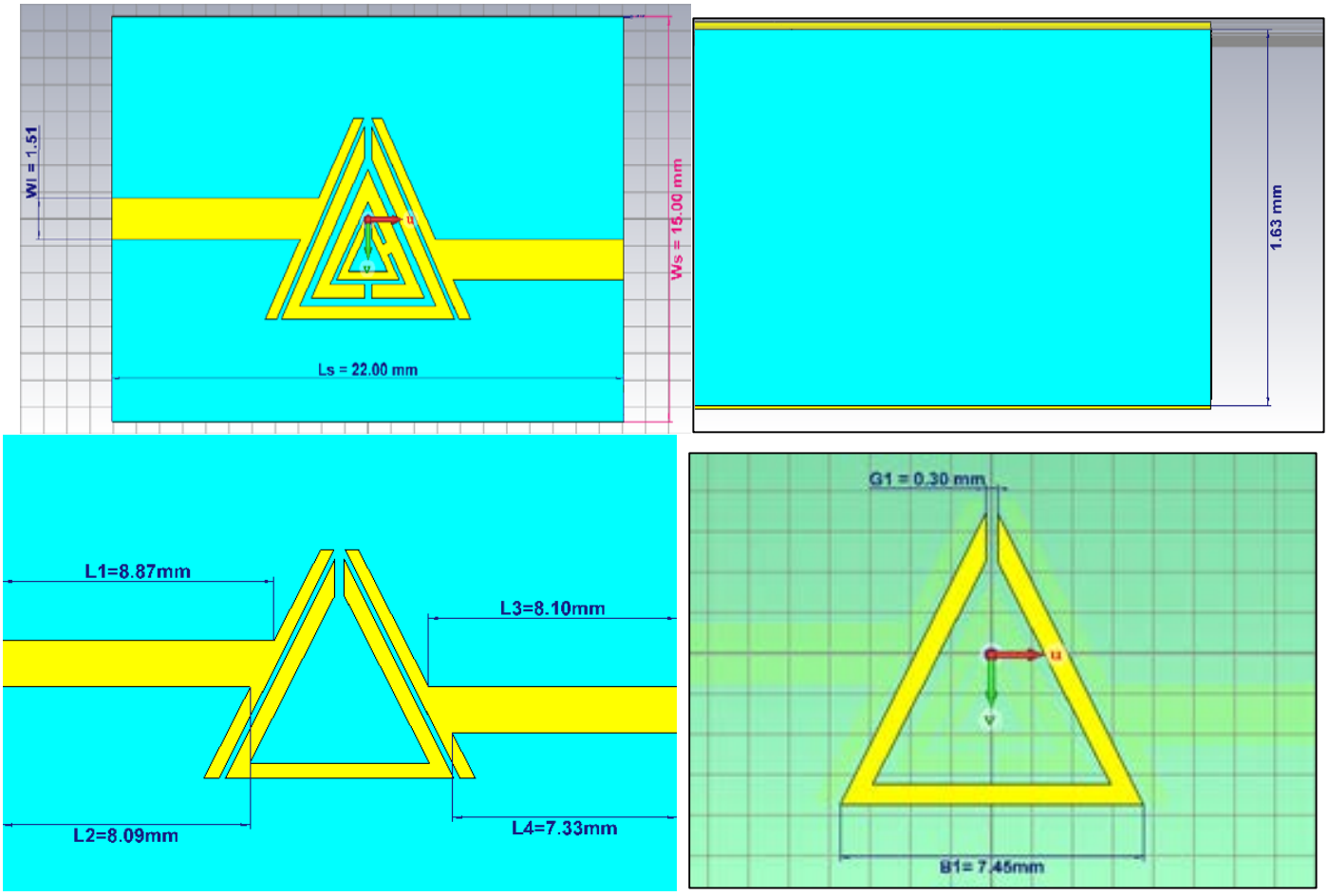

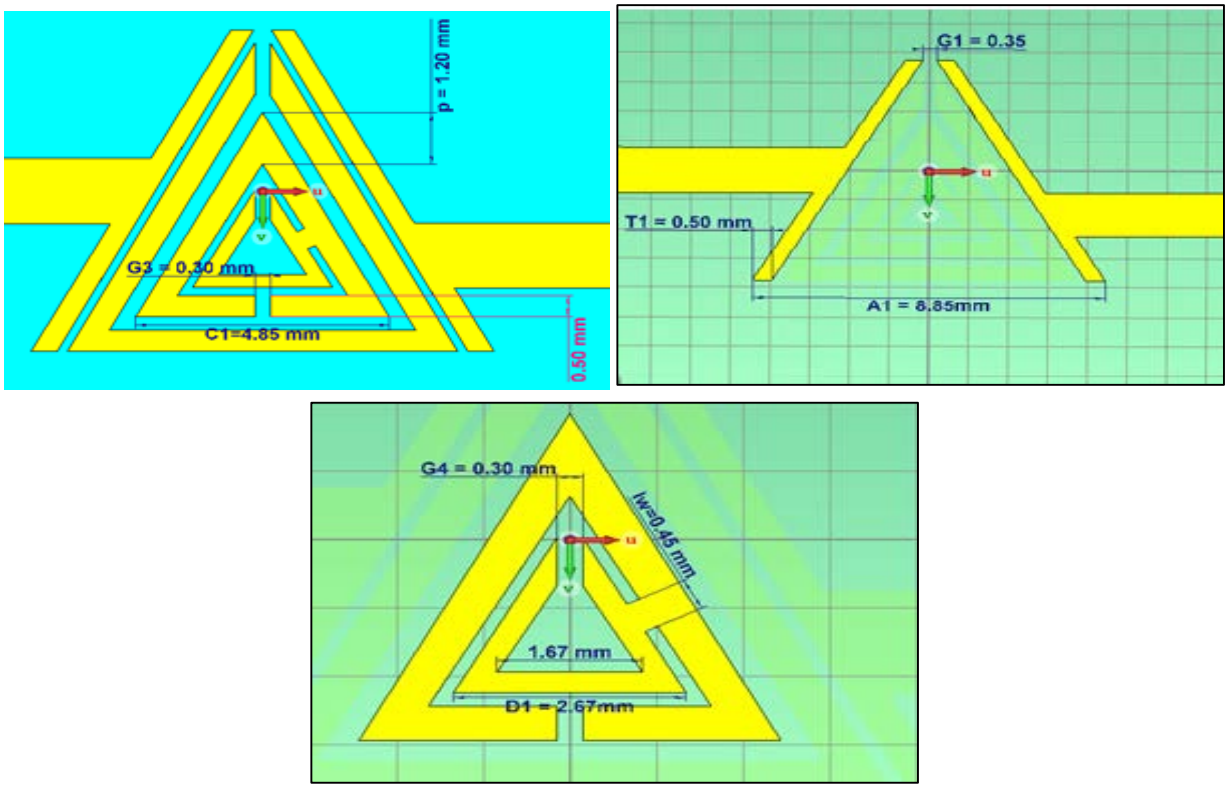

Figure 3. 25 The dimensions of the design

Table 3.1 the dimension of the design

Dimension	Description	Value in mm
Ls	Length of the substrate	22
Ws	Width of the substrate	15
Ts	Thickness of the substrate	1.63
Wl	Width of the line	1.51
T	Thickness of the line and ground plane	0.035
A1	Length of the base of the outer triangle of 1st SRR	8.85
B1	Length of the base of the inner triangle of 1st SRR	7.45
C1	Length of the base of the outer triangle of 2ndSRR	4.85

D1	Length of the base of the inner triangle of 2nd SRR	2.67
D2	Length of the base of the inner line in the 2nd SRR	1.67
G1	Gap 1	0.35
G2	Gap 2	0.3
G3	Gap 3	0.3
G4	Gap 4	0.3
p	Thickness at the top of triangle 3 of 2nd SRR	1.2
lw	Width of the link	0.45
L1	_	8.87
L2	_	8.09
L3	_	8.1
L4	_	7.33

3.3.2 Performance of the filter:

The performances of the filter are summarized in Table 3-2.

Table 3.2. filter performances

Band	Band 1	Band 2
Central frequencies in GHz	3.5 GHz	5.8
The insertion loss in dB	-1.5	-2.9
S21max in dB	+33	+33
Stop band at -15dB rejection	3.9 GHz to 4.6 GHz	6 Ghz to 6.8 GHz

Bandwidth	0.39 Ghz	0.05 Ghz

3.4 Surface current distribution:

At frequencies in the pass band the current is distributed in all of the filter as shown in figure 3-26 and 3-27:

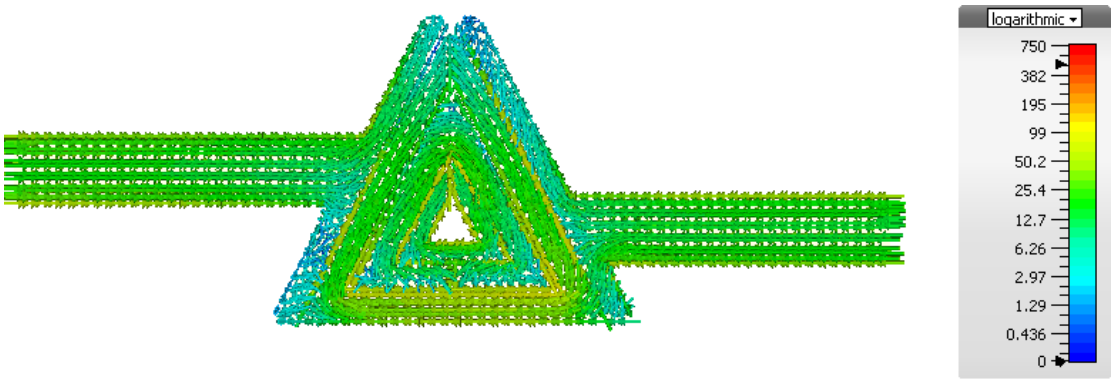

Figure 3. 26 Current density at 3.5 GHz

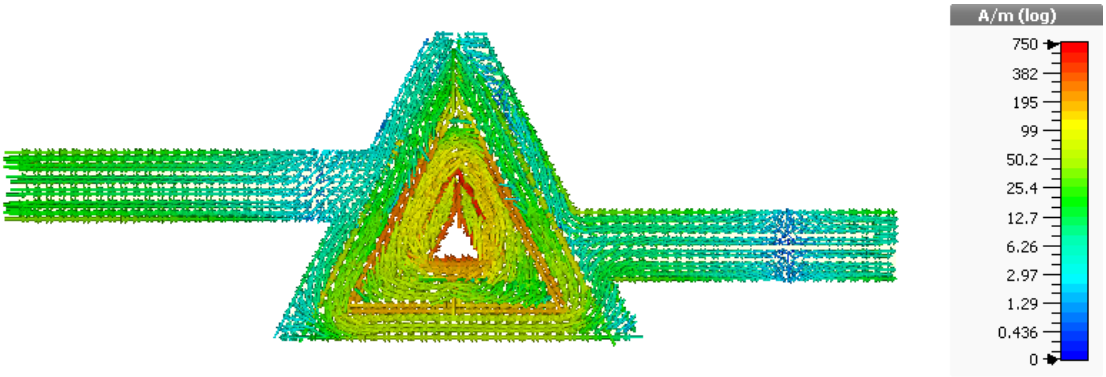

Figure 3. 37 Current density at 5.8 GHz

Whereas at frequencies in the stop band the current is concentrated in the right part of the filter. the following figure display current distributions at as shown in figures

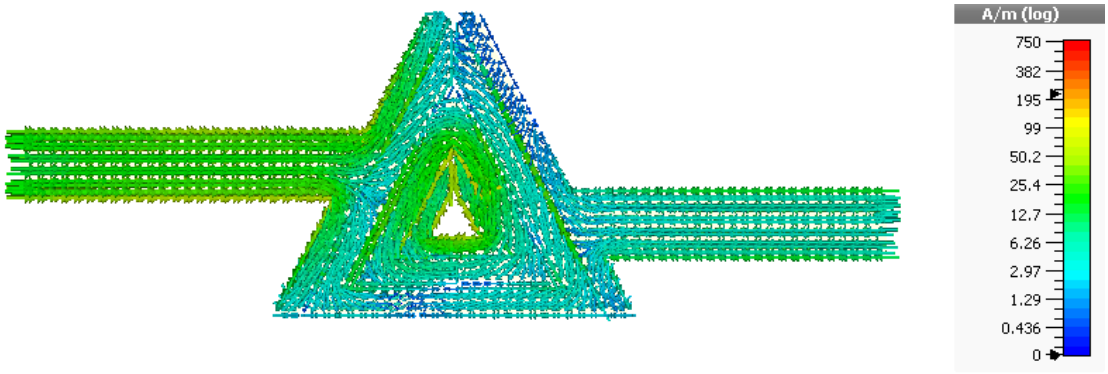

Figure 3. 28 Current density at 5 GHz

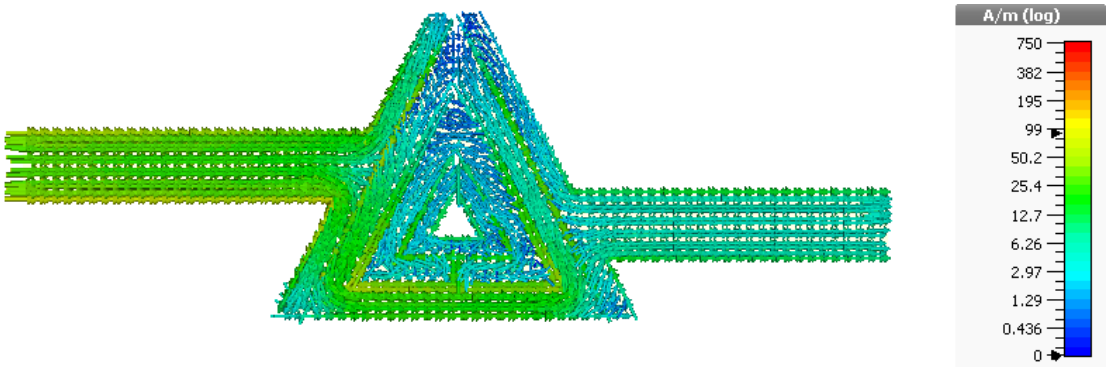

Figure 3. 29 current density at 1.9 GHz

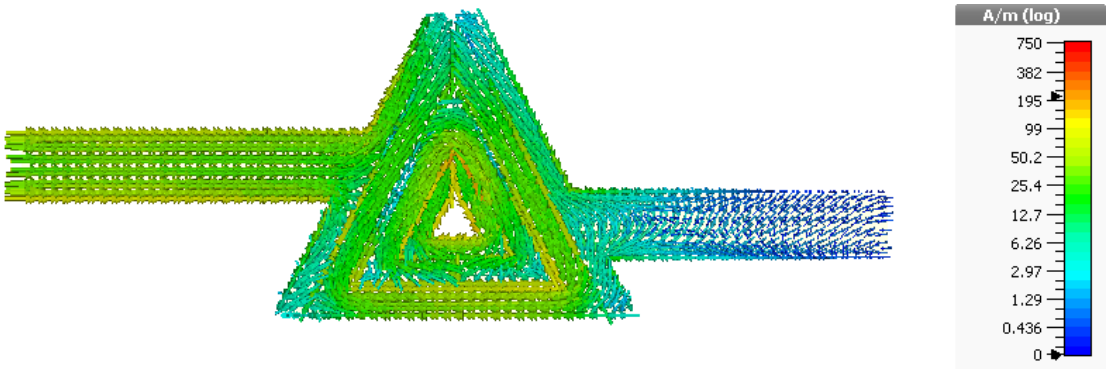

Figure 3. 30 Current density at 4.1 GHz

3.5 The metamaterial property:

To simulate the unit cell, we separate it for the microstrip line, and we omit the copper ground plane from the design, lastly, we set the boundary conditions as shown in figure (3-30)

We remark when we simulate the unit cell we get a range of frequencies [3.4 GHz to 4.1 GHz] where the relative permittivity and the relative permeability are negative. So the cell behaves as a double negative metamaterial as shown in the following figures (3-31) and (3-32).

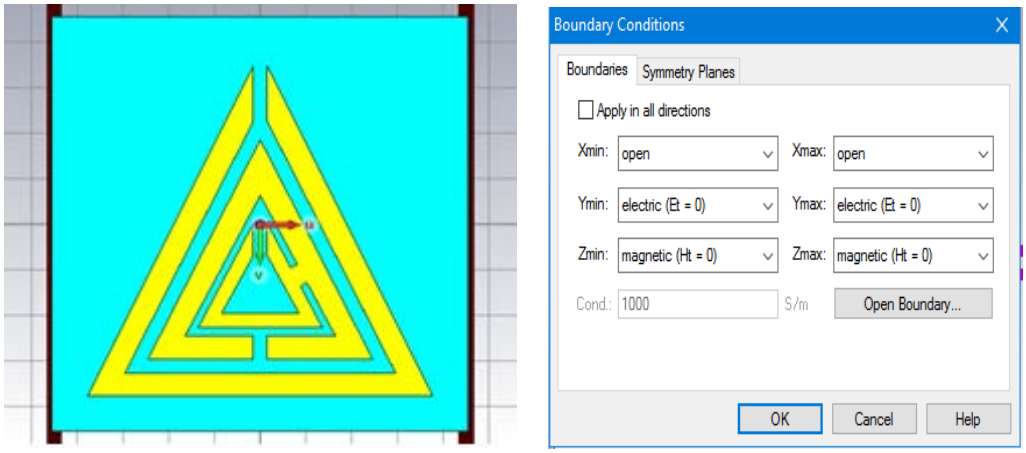

Figure 3. 31 3D model and boundary conditions for the metamaterial cell simulation

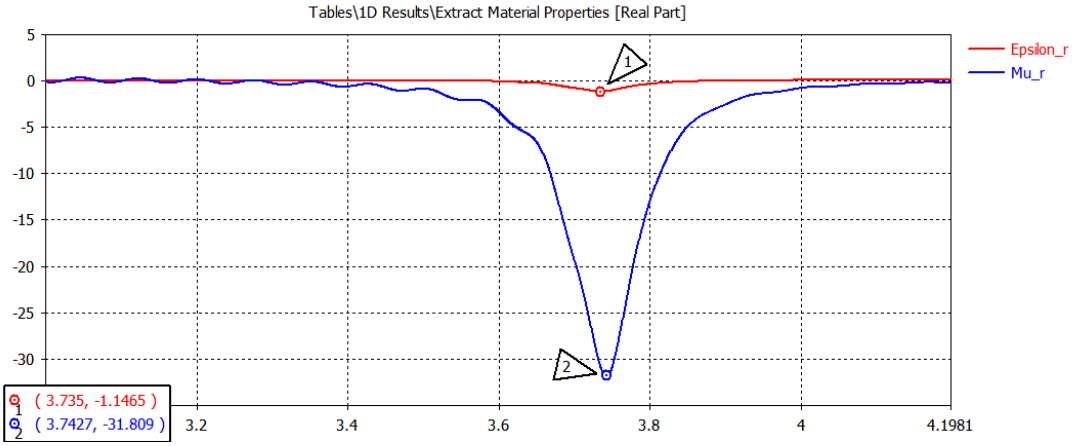

Figure 3. 32 real part of relative permittivity and permeability graphs for the unit cell

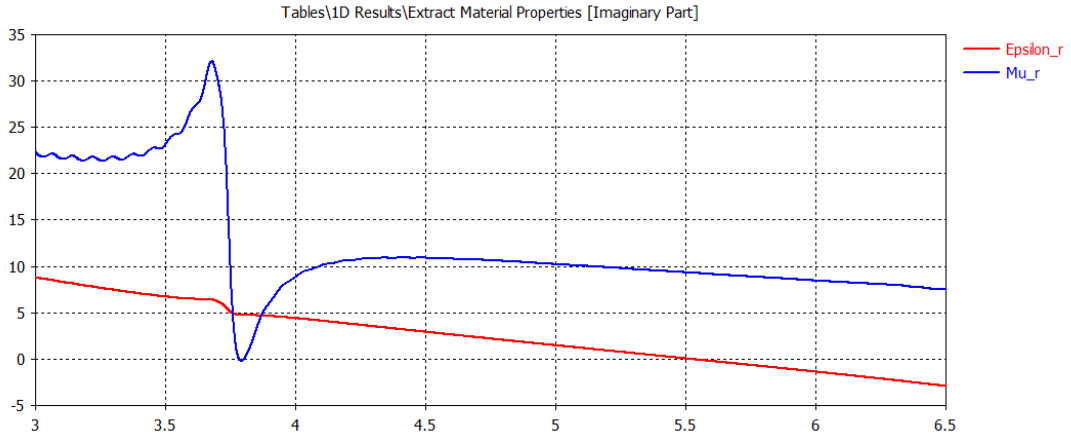

Figure 3. 33 imaginary part of relative permittivity and permeability graphs for the unit cell

3.6 Conclusion:

In this chapter a metamaterial-based filter was designed and tuned to serve in WiMAX communication system, we chose the triangular shape instead of more famous shapes like the circular and rectangular shapes as in [31] and [32], the steps of realization were displayed, then the S parameter results were displayed. The performance was somewhat satisfactory but the losses could not be 100% decreased, it was also shown that the results gotten were optimal by varying many parameters. we remarked that a DNG metamaterial behaviour is observed in the range [3.4 GHz – 4.1 GHz].

Conclusion

In this work, a dual-band bandpass filter (BPF) based on a triangular metamaterial unit cell was designed using CST Microwave simulation software. This filter was tuned to have two passbands, at frequencies 3.5 GHz and 5.8 GHz, intended for WIMAX communication system.

This work has been organized as follows:

A literature of review of the theory of filters has been introduced in the first chapter. The second chapter gives a general idea on Metamaterials. In the last one, a design of dual-band BPF using metamaterial property with low insertion loss and compact size was introduced.

It was shown that the proposed filter was precisely tuned to have narrow passbands with central frequencies at 3.5 GHz and 5.8 GHz. Good performance was obtained in terms of return and insertion losses.

As future work, the following points are suggested:

1. It would be interesting to fabricate and measure the performance of the presented dual-band BPF.
2. The second goal would be the circuit modeling of the proposed filter.

Finally, we hope that this work will be beneficial for further microwave projects in general and for filter applications in particular.

Appendix a

Cst microwave studio:

CST microwave studio (CST MWS) is a powerful tool for 3d electromagnetic EM simulation of high frequency components. CST MWS offers unparalleled performance, making it first choice in leading R&D departments.

CST MWS enables the fast and accurate analysis of high frequency devices such as antennas, filters , couplers , planar ,and multi-layer structures and S1 and EMC effects . Exceptionally user friendly, CST MWS quickly gives an insight into the EM behaviour of high frequency designs.

Overview of the interface

After the module has started you will see the user interface of CST MICROWAVE STUDIO. Now let us have a closer look at the various user interface elements:

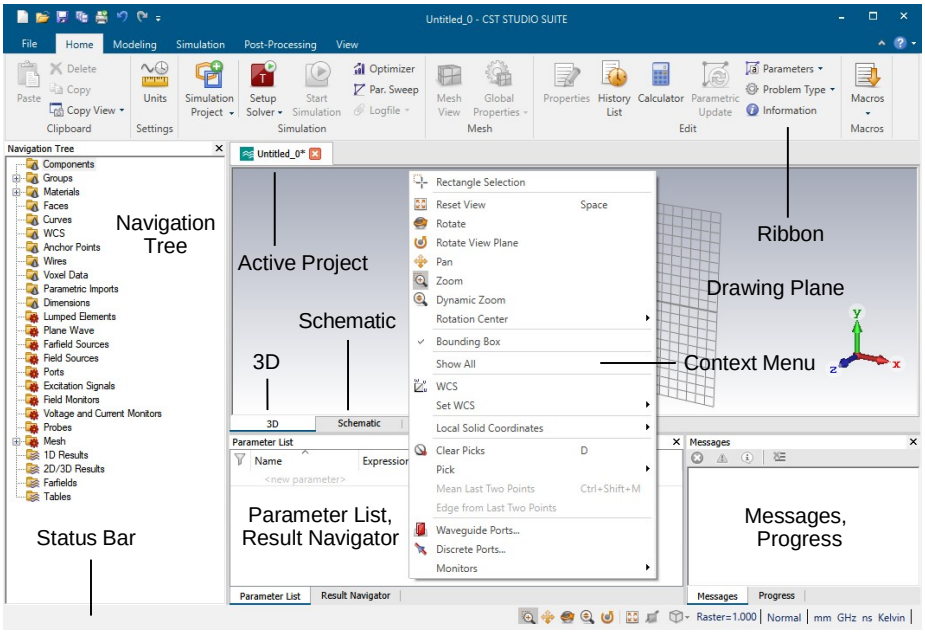

Users of CST MWS can choose between six powerful solver modules each offering distinct advantages in their own domains.

The Ribbon command bar organizes all user interface controls in a series of tabs. It is a replacement for the classical menus and toolbars:

APPENDIX A

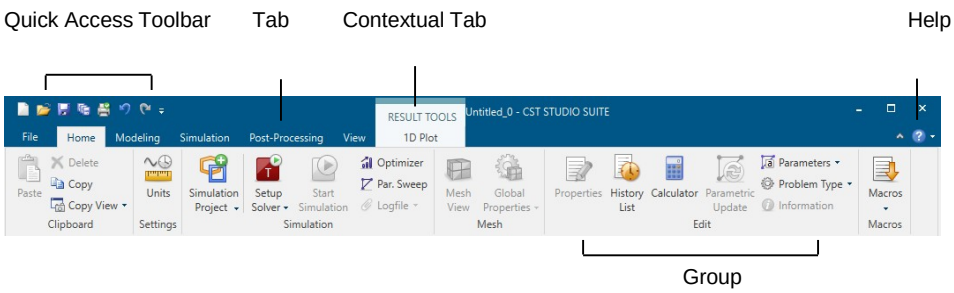
Quick Access Toolbar
Tab
Contextual Tab
Help
RESULT TOOLS
Untitled_0 - CST STUDIO SUITE
File
Home
Modeling
Simulation
Post-Processing
View
1D Plot
Paste
Delete
Copy
Copy View
Clipboard
Units
Settings
Simulation Project
Setup Solver
Start Simulation
Optimizer
Par. Sweep
Logfile
Simulation
Mesh View
Global Properties
Mesh
Properties
History List
Calculator
Parametric Update
Parameters
Problem Type
Information
Edit
Macros
Macros
Group

References

[1] R. M. Fano and A. W. Lawson, *Microwave Transmission Circuits*, ser. M.I.T. Rad. Lab.. New York: McGraw-Hill, 1948, vol. 9, ch. 9, 10.

[2] Ian C. Hunter, Laurent Billonet, Bernard Jarry, and Pierre Guillon, Microwave Filters—Applications and Technology IEEE transactions on microwave theory and techniques, vol. 50, no. 3, march 2002

[3] Veselago, Viktor & Lebedev, P. (1968). Veselago, V. G. The electrodynamics of substances with simultaneously negative values of permittivity and permeability and. Soviet Physics Uspekhi. 1968.

[4] Kerry Lacanette "A Basic Introduction to Filters and Active, Passive,and Switched-Capacitor" National Semiconductor Application Note 779 April 1991

[5] J.-K. Xiao, *Defected Microstrip Structure*, Wiley Encyclopedia of Electrical and Electronics Engineering, 2013.

[6] David M. Pozar " Microwave Engineering, fourth edition " 1998.

[7] F. Caspers "RF engineering basic concepts: S-parameters" CERN, Geneva, Switzerland . July 2005.

[8] Darine Kaddour. "Conception et Réalisation de filtres RF passe-bas à structures périodiques et filtres Ultra Large Bande, semi-localisés en technologie planaire", Université Joseph- Fourier- Grenoble I, 2007.

[9] Christophe Caloz, Tatsuo Itoh,"Electromagnetic metamaterials transmission line theory and microwave applications", April 4, 2005.

[10] Jia-Shenghong, M.J.Lancaster "Microstrip Filters for rf and microwave applications" , 2001.

[11] R. A. Shelby, D. R. Smith, S. C. Nemat-Nasser, and S. Schultz "Microwave transmission through a two-dimensional, isotropic, left-handed metamaterial",2001

[12] "Developing a compact microwave filter using metamaterials ".

[13] Ricardo Marques,Ferran Martin,Mario Sorolla "Metamaterials with Negative Parameters".

[14] Christophe Caloz AND Tatsuo Itoh,"metamaterials in high frequency electronics", 2005.

[15] I.A. Buriak1, V.O. Zhurba1, G.S. Vorobjov1, V.R. Kulizhko1, O.K. Kononov1

Oleksandr Rybalko, "metamaterials theory, classification and application strategies" December, 23rd 2016.

[16] L. Solymar, E. Shamonina, "waves in metamaterials", June 24th, 2014.

[17] Kyriazidou, Chryssoula & Contopanagos, Harry & Alexopoulos, Nicolaos. "Theory and Design of Metamorphic Materials" December 2017.

[18] Richard.W.Ziolkowski"design fabrication and testing of DNG metamaterials" July 2003.

[19] "Transmission characteristics of bianisotropic metamaterials based on omega shaped metallic inclusions» September, 14th 2007

[20] S. I. Maslovski, P. M. T. Ikonen, I. Kolmakov, S. A. Tretyakov, and M. Kaunisto, "Artificial Magnetic Materials Based on the New Magnetic Particle: Metasolenoid," *Progress in Electromagnetics Research*, Vol. 54, 61-81, 2005.

[21] P. Markoš and C. M. Soukoulis " Numerical studies of left-handed materials and arrays of split ring resonators» March ,7th 2002

[22] Ian C. Hunter ."Theory and Design of Microwave Filters" The Institution of Engineering and Technology (2001)

[23] H. Issa. "Miniaturisation des lignes de propagation microondes en technologies circuit imprimé et CMOS - Application a` la synthèse de filtres", Micro et nanotechnologies/Micro´électronique. UJF, 2009.

[24] M.Meeloon, E. Nugoolcharoenlap, P. Akkaraekthalin, UWB Bandpass Filters with Sharp Rejection using Folded Defected Ground Structure, King Mongkut's University of Technology, North Bangkok Thailand.

[25] Agilent Technologies Agilent EEsof EDA Advanced Design System Circuit Design handbook .

[26] Tengfei Y, Xiao-H T, Junfeng W. A novel quad-band bandpass filter using short loaded E-shaped resonators. IEEE Microw and Wirel Compon Lett. 2015; 25:508-510.

[27] Wei J, Wei S, Tengxing W, Yong MH, Yujia P. GuoanWang: compact dual-band filter using open/short stub loaded stepped impedance resonators (OSLSIRs/SSLSIRs). IEEE Microw and Wirel Compon Lett. 2016; 26:1531-1309.

[28] Chu-Y C, Cheng-Y H. A simple and effective method for micro-strip dual-band filters design. IEEE Microw and Wirel Compon Lett. 2006; 16:246-248.

[29] Hayati M, Khajavi A, Abdi H. A miniaturized microstrip dual-band Bandpass filter using folded UIR for multimode WLANs.ACES - App Comput Electrom Society J. 2013;28:35-40.

[30] Kaijun S, Fan Z, Yong F. Miniaturized dual-band bandpass filter with good frequency selectivity using SIR and DGS. Intern J of Electronics and Communic (AEÜ). 2013; 68:384 387.

[31] Makimoto M, Yamashita S. Microwave Resonators and Filters for Wireless Communication, Theory, Design and Application.Berlin: Springer; 2001.

[32] CST STUDIO SUITE 2018/Online Help/cst _studio_suite_help.htm

[33] Abdallah Chahadih , Abbas Ghaddar, Mokhtar Zehar, Derek Abbott, Christophe Fumeaux, and Tahsin Akalin "Metamaterial-Inspired Bandpass Filters for Terahertz Surface Waves on Goubau Lines" .

[34] XIN HU "Some studies on metamaterial transmission lines and their applications", Doctoral Thesis in Electromagnetic Theory Stockholm, Sweden 2009

People's Democratic Republic of Algeria
Ministry of Higher Education and Scientific Research

University M'Hamed
BOUGARA - Boumerdes

Institute of Electrical and
Electronic Engineering

Department of Electronics

Authorization for Final Year Project Defense

Academic year: 2019/2020

The undersigned supervisor: **Prof.M..Challal**
authorizes the student(s):

Zaboub Oussama Option **Telecommunications**

Debili Seif El Islam Option **Telecommunications**

to defend his / her / their final year Master program project entitled:

Design of a metamaterial dual-band bandpass filter for Wimax applications

during the ☐ June ☐ September session.

Date: .. / .. / 2020

The Supervisor The Department Head